Robust quantum walk search without knowing the number of marked vertices

Yongzhen Xu, Delong Zhang, and Lvzhou Li*

Institute of Quantum Computing and Computer Theory, School of Computer Science and Engineering, Sun Yat-sen University, Guangzhou 510006, China

(Received 7 April 2022; accepted 19 October 2022; published 14 November 2022)

There has been a very large body of research on searching a marked vertex on a graph based on quantum walks, and Grover's algorithm can be regarded as a quantum walk-based search algorithm on a special graph. However, the existing quantum walk-based search algorithms suffer severely from the soufflé problem, which mainly means that the success probability of finding a marked vertex could shrink dramatically, even to zero, when the number of search steps is greater than the right one, thus heavily reducing the robustness and practicability of the algorithm. Surprisingly, while the soufflé problem of Grover's algorithm has attracted enough attention, how to address this problem for general quantum walk-based search algorithms is missing in the literature. Here we initiate the study of overcoming the soufflé problem for quantum walk-based search algorithms by presenting a quantum walk-based search framework that achieves robustness without sacrificing the quantum speedup. In this framework, for any adjustable parameter ϵ, the quantum algorithm can find a marked vertex on an N-vertex *complete bipartite graph* with probability at least $1-\epsilon$, whenever the number of search steps h satisfies $h \geqslant \ln(\frac{2}{\sqrt{\epsilon}})\sqrt{N}+1$. Note that the algorithm need not know the exact number of marked vertices. Consequently, we obtain quantum search algorithms with stronger robustness and practicability.

DOI: 10.1103/PhysRevA.106.052207

I. INTRODUCTION

Quantum walks, the analogs of classical random walks in the quantum realm, were first introduced by Aharonov *et al.* [1] in 1993. In the last nearly 30 years, much progress about quantum walks has been made from theory to experiments. Quantum walks have become a basic tool for designing quantum algorithms to settle a series of problems such as element distinctness [2], triangle finding [3], quantum backtracking [4], and so on [5–9]. Furthermore, they are a universal model of quantum computation [10,11]. In the aspect of experiment study, various hardware platforms have been used to demonstrate results of quantum walks, e.g., Refs. [12–15]. There are two types of quantum walks: discrete-time quantum walks [16–20] and continuous-time quantum walks [21,22]. In this paper, we are concerned with the discrete-time model.

A central topic in quantum walk-based algorithms is to develop efficient quantum algorithms for searching a marked vertex on a graph. This idea was initially proposed in 2003 by Shenvi *et al.* [23] who constructed a quantum walk search algorithm on the Boolean hypercube for finding a marked item in a data set. Later, Ambainis *et al.* [24] proposed search algorithms based on quantum walks on d-dimensional lattices ($d \geqslant 2$). A major breakthrough was that Ambainis [2] obtained the optimal query complexity of the element distinctness problem by employing quantum walk search on Johnson graphs. In 2004, Szegedy [25] studied the general theory of quantum walk search algorithms from the point of view of Markov chains. In this direction, a series of work [26–29] was put forward for searching a marked state in different Markov chains using phase estimation, interpolated quantum walks, and quantum fast-forwarding.

Grover's algorithm can be regarded as a quantum walk search algorithm on a complete graph with a self-loop on every vertex [24]. As pointed out by Brassard [30], Grover's quantum searching technique suffers from the soufflé problem [31]. As a result, if the exact number of marked items is not known in advance, then one does not know when to stop the search iteration. Even if the number is known, the success probability of the algorithm could shrink dramatically when the number of query steps is greater than the right one, as shown in Fig. 1(a). Two strategies are often used to deal with the unknown number of solutions. One method is the exponential search algorithm [32] in which the number of iterations increases slowly but exponentially. Another strategy is to employ quantum counting [33] to estimate the number of marked items. However, they are still essentially an oscillatory Grover search and fail to completely solve the soufflé problem. From a search perspective, the success probability of getting a marked item should not shrink (at least not shrink dramatically) as the number of search steps increases.

To overcome the soufflé problem, Grover [34] proposed a fixed-point quantum search algorithm that converges monotonically to the target, i.e., avoid overcooking by always amplifying the marked items [as shown in Fig. 1(b)]. Yet, a price paid for this monotonicity is that the quadratic speedup of the original quantum search is lost. In 2014, Yoder *et al.* [35] presented a quantum search algorithm that achieves both goals—the search cannot be overcooked and also achieves optimal time scaling, a quadratic speedup over classical unordered search. This algorithm does not require that the error

*Corresponding author: lilvzh@mail.sysu.edu.cn

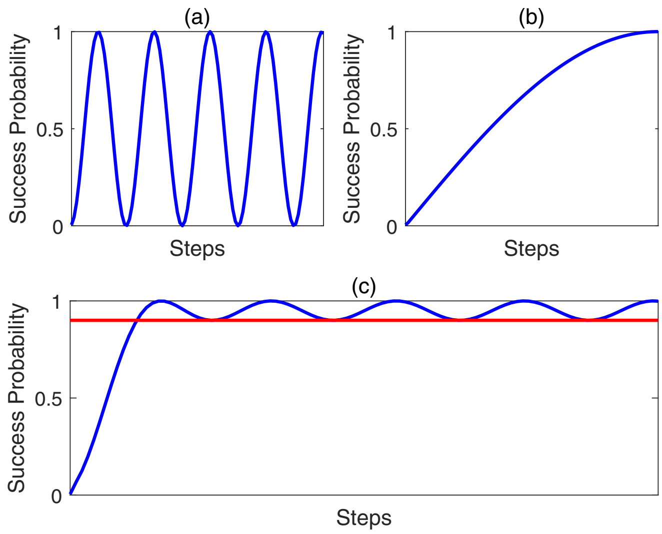

FIG. 1. The success probability of finding a marked item as a function of steps in three search models. (a) Grover-type oscillatory search. (b) Fixed-point Search. (c) Robust search.

monotonically improves, but ensures that the error becomes bounded by a tunable parameter ϵ, as shown in Fig. 1(c). Thus, this leads to a more robust quantum search algorithm. In addition, the fixed-point quantum search was discussed from an information perspective by Cafaro [36] and from the view of analog quantum search with suitable Hamiltonians specifying time-dependent two-level quantum systems by Cafaro and Alsing [37]. Currently, various quantum walk search algorithms also suffer from the soufflé problem. To the best of our knowledge, there has been no work considering how to avoid the sofflé problem from the perspective of quantum walk search. Actually, the problem becomes more challenging than in Grover's quantum search. There are at least three reasons for the difficulty of addressing the soufflé problem for quantum walk search algorithms. First, the search space is more complicated because of the diversity of topological structure of graphs. Second, more operations are involved in quantum walk search. Third, it is generally difficult to get an analytical expression for the success probability and to analyze the computational complexity of a quantum walk search algorithm.

Our contributions

This paper considers how to address the soufflé problem confronted by quantum walk search algorithms. We take a step in this direction by designing a robust quantum walk search algorithm on complete bipartite graphs (NOT complete graphs). Note that this kind of graph was extensively studied in quantum walk search algorithms [38–41]. The robustness feature of our algorithm ensures that for an N-vertex complete bipartite graph with marked vertices but without knowing the number of marked vertices, if the number of search steps h satisfies $h \geqslant \ln(\frac{2}{\sqrt{\epsilon}})\sqrt{N}+1$, then the algorithm will output a marked vertex with probability at least $1-\epsilon$ for any given $\epsilon \in (0,1]$ (the formal statement can be found in Theorem 1). Thus, the algorithm both avoids overcooking and keeps quadratic speedup over classical ones. Also note that our algorithm need not know the number of target vertices.

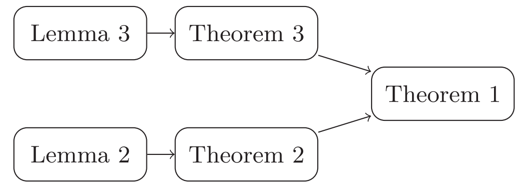

FIG. 2. The relationship among the theorems and technical lemmas.

To obtain the above result, some nontrivial technical treatments are required. (1) First, compared to Grover's algorithm, the coined quantum walk search framework has two subsystems and three operations. Thus, what operations should be adjusted to create a robust version is not obvious, and we show that a model with two parameterized operations is sufficient. (2) Second, while one needs only consider essentially a two-dimensional state space for Grover's algorithm, higher dimensional state spaces are involved in quantum walk search and thus it is not even easy to track the state of the quantum system. Luckily, we reveal some crucial observations (especially Lemma 4) to simplify the expression of the final state. It is worth noting that these observations are specific to quantum walks and are not seen in the robust version of Grover's algorithm [35]. We think that these technical treatments may inspire the analysis of robust quantum walk search on other general graphs.

Theorem 1. Given an N-vertex complete bipartite graph with marked vertices but without knowing the number of marked vertices, there exists a quantum walk-based algorithm such that if the number of search steps h satisfies $h \geqslant \ln(\frac{2}{\sqrt{\epsilon}})\max(\sqrt{N_l},\sqrt{N_r})+1$, then the algorithm will output a marked vertex with probability at least $1-\epsilon$ for any given $\epsilon \in (0,1]$, where N_l (N_r) is the number of the left (right) vertices in the complete bipartite graph.

The relationship among the theorems and technical lemmas obtained in this paper are depicted in Fig. 2. Theorem 1 states the main result of this paper, which comes from Theorems 2 and 3, which corresponds, respectively, to the two cases: the marked vertices are on one side and on two sides of a complete bipartite graph. Furthermore, Lemma 2 (Lemma 3) is crucial for proving Theorem 2 (Theorem 3), with proofs given in Sec. IV and Appendices A–D.

II. PRELIMINARIES

A. Graph notation

Let $G=(V,E)$ be an undirected, unweighted graph with $N=|V|$ vertices and $m=|E|$ edges. An edge between u and v is denoted by (u,v). For $u\in V$, $\deg(u)=\{v:(u,v)\in E\}$ denotes the set of neighbors of u, and the degree of u is denoted as $d_u=|\deg(u)|$. A bipartite graph is represented as $G=(V=\{V_l\cup V_r\},E)$, where V_l (V_r) denotes the set of vertices on the left (right) side, with $V_l\cap V_r=\emptyset$. We use N_l and N_r to denote the number of left and right vertices, respectively. The number of the marked vertices on the left (right) side is n_l (n_r). A complete bipartite graph is a bipartite graph where

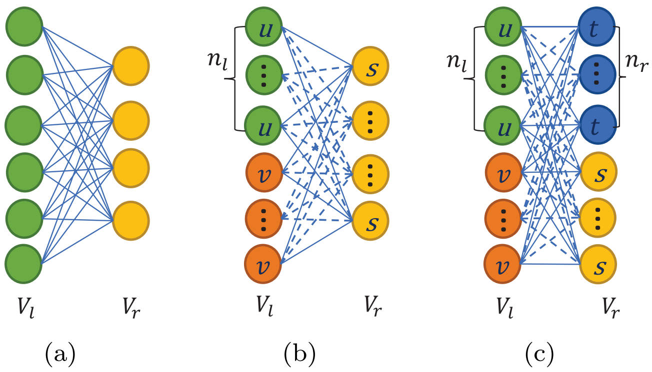

FIG. 3. (a) A complete bipartite graph G with ten vertices. (b) An N-vertex complete bipartite graph with the marked vertices denoted by u on the left, the unmarked vertices denoted by v on the left, and s on the right. (c) An N-vertex complete bipartite graph with the marked vertices denoted by u on the left and t on the right, the unmarked vertices denoted by v on the left and s on the right.

every vertex on the left side is connected to every vertex on the right side. For example, a complete bipartite graph in Fig. 3(a) contains six vertices on the left side and four vertices on the right side.

B. Coined quantum walk

In this model, the walker's Hilbert space associated with an N-vertex graph $G = (V, E)$ is $\mathbb{H}^{N^2} = \text{span}\{|uv\rangle, u, v \in V\}$, where u is the position and v is the coin value representing one neighbor of u. The evolution operator of the coined quantum walk at each step is $U_{\text{walk}} = SC$, where the flip-flop shift operator S is defined as $S|uv\rangle = |vu\rangle$, and the coin operator is $C = \sum_u |u\rangle\langle u| \otimes C_u$. The Grover diffusion coin operator C_u often used is $C_u = 2|s_u\rangle\langle s_u| - I$, where $|s_u\rangle = \frac{1}{\sqrt{d_u}} \sum_{v\in\deg(u)} |v\rangle$.

Given the initial state $|\Psi_0\rangle$, the walker's state after h steps is $|\Psi_h\rangle = U^h_{\text{walk}}|\Psi_0\rangle$.

C. Quantum walk search

In the quantum walk search framework, to find a marked vertex in a graph, the query oracle Q is given by

$$Q|uv\rangle = \begin{cases} -|uv\rangle & \text{if } u \text{ is marked} \\ |uv\rangle & \text{if } u \text{ is not marked.} \end{cases}$$

The evolution operator corresponding to one step of the quantum walk search is $U = SCQ$.

Given the initial state $|\Psi_0\rangle$, the walker's state after t steps is $|\Psi_t\rangle = U^t|\Psi_0\rangle$. Finally, the first register is measured and the measurement result is output.

D. Chebyshev polynomial

The Chebyshev polynomials of the first kind $T_n(x)$ are defined by initial values $T_0(x) = 1$, $T_1(x) = x$, and for an integer $n \geqslant 2$:

$$T_n(x) = 2xT_{n-1}(x) - T_{n-2}(x).$$

The trigonometric identity $T_n(x) = \cos[n \arccos(x)]$ is well-known.

A result of one quasi-Chebyshev polynomial implied in Ref. [35] is stated in the following lemma.

Lemma 1. Let $x = \cos(\theta)$ for $\theta \in [0, 2\pi]$. Let $h \geqslant 3$ be an odd integer. One quasi-Chebyshev polynomial $a_k(x)$ is defined by initial values $a_0(x) = 1$, $a_1(x) = x$, and for $k = 2, \ldots, h$,

$$a_k(x) = x(1 + e^{-i(\zeta_k - \zeta_{k-1})})a_{k-1}(x) - e^{-i(\zeta_k - \zeta_{k-1})}a_{k-2}(x).$$

When $\zeta_{k+1} - \zeta_k = (-1)^k\pi - 2\text{arccot}\,(\tan(k\pi/h)\sqrt{1-\gamma^2})$ for $k = 1, \ldots, h-1$, where $\gamma = \frac{1}{\cos[\frac{1}{h}\arccos(\frac{1}{\sqrt{\epsilon}})]}$ with $\epsilon \in (0, 1]$, we have $a_h(x) = \frac{T_h(x/\gamma)}{T_h(1/\gamma)}$ with $T_h(1/\gamma) = 1/\sqrt{\epsilon}$.

III. ROBUST QUANTUM WALK SEARCH ON COMPLETE BIPARTITE GRAPHS

As mentioned before, the already existing quantum walk search algorithms suffer from the soufflé problem. Thus, this paper is devoted to addressing this problem by considering the case of searching a marked vertex in a complete bipartite graph. For that, first the coin operator C and the query oracle Q have to be adjusted, but the flip-flop shift operator S can remain unchanged. The new evolution operator of one search step is

$$U(\alpha, \beta) = SC(\alpha)Q(\beta), \tag{1}$$

where the coin operator C is changed to

$$C(\alpha) = \sum_u |u\rangle\langle u| \otimes [(1 - e^{-i\alpha})|s_u\rangle\langle s_u| - I]$$

and the query oracle Q is replaced by

$$Q(\beta)|uv\rangle = \begin{cases} e^{i\beta}|uv\rangle & \text{if } u \text{ is marked} \\ |uv\rangle & \text{if } u \text{ is not marked.} \end{cases}$$

When $\alpha = \beta = \pm\pi$, this model becomes the original quantum walk search [24,39].

The algorithm of search on a complete bipartite graph is given in Algorithm 1. In the input phase, according to the information of marked vertices and a tunable parameter ϵ, the number of search steps h is required to satisfy

$$h \geqslant \begin{cases} \ln\left(\frac{2}{\sqrt{\epsilon}}\right)\sqrt{\frac{N_l}{n_l}} + 1 & \text{marked vertices in one side with } n_l \geqslant 1, n_r = 0 \\ \ln\left(\frac{2}{\sqrt{\epsilon}}\right)\max\left(\sqrt{\frac{N_l}{n_l}}, \sqrt{\frac{N_r}{n_r}}\right) + 1 & \text{marked vertices in two sides with } n_l \geqslant 1, n_r \geqslant 1 \\ \ln\left(\frac{2}{\sqrt{\epsilon}}\right)\max(\sqrt{N_l}, \sqrt{N_r}) + 1 & \text{without knowing the number and any arrangement of marked vertices.} \end{cases} \tag{2}$$

The parameters α, β are given by

Algorithm 1 Robust quantum walk search

Inputs: An N-vertex complete bipartite graph with marked vertices, $\epsilon \in (0, 1]$, and the number of search steps h.
Outputs: A marked vertex x_0 [if h satisfies Eq. (2), it outputs a marked vertex with probability at least $1-\epsilon$].
Procedure:
1. Prepare the initial state $|\Psi_0\rangle = \frac{1}{\sqrt{2N_lN_r}}(\sum_u |u\rangle \otimes \sum_{v\in\deg(u)} |v\rangle)$.
2. Apply $U(\alpha_1, \beta_1), \dots, U(\alpha_h, \beta_h)$ in turn, where the parameters α_i, β_i are determined by Eqs. (3) and (4).
3. Measure the first register in the computational basis. If the result vertex is not marked, then the second register is measured. Output the measurement result.

Case 1: h is odd:

$$\alpha_k = \begin{cases} -\beta_{h+2-k} = 2\text{arccot}\left(\tan\left(\frac{k\pi}{h}\right)\sqrt{1-\gamma^2}\right) & k = 2, 4, \dots, h-1 \\ -\beta_{h-k} = 2\text{arccot}\left(\tan\left(\frac{(k-1)\pi}{h}\right)\sqrt{1-\gamma^2}\right) & k = 3, 5, \dots, h \\ \alpha_1 \text{ and } \beta_h \text{ can be any value,} \end{cases} \tag{3}$$

where $\gamma^{-1} = \cos[\frac{1}{h}\arccos(\frac{1}{\sqrt{\epsilon}})]$.

Case 2: h is even:

$$\alpha_k = -\beta_{h+1-k} = \begin{cases} 2\text{arccot}\left[\tan\left(\frac{k\pi}{h+1}\right)\sqrt{1-\gamma_1^2}\right] & k = 2, 4, \dots, h \\ 2\text{arccot}\left[\tan\left(\frac{(k-1)\pi}{h-1}\right)\sqrt{1-\gamma_2^2}\right] & k = 3, 5, \dots, h-1 \\ \alpha_1 \text{ and } \beta_h \text{ can be any value,} \end{cases} \tag{4}$$

where $\gamma_1^{-1} = \cos[\frac{1}{h+1}\arccos(\frac{1}{\sqrt{\epsilon}})]$ and $\gamma_2^{-1} = \cos[\frac{1}{h-1}\arccos(\frac{1}{\sqrt{\epsilon}})]$.

In the first step, the initial state $|\Psi_0\rangle = \frac{1}{\sqrt{2N_lN_r}}(\sum_u |u\rangle \otimes \sum_{v\in\deg(u)} |v\rangle)$ is prepared. Then, $U(\alpha_1, \beta_1), \dots, U(\alpha_h, \beta_h)$ with appropriate parameters are applied to $|\Psi_0\rangle$ in turn. The whole operator that performs h steps is $\Gamma_h = U(\alpha_h, \beta_h)...U(\alpha_1, \beta_1)$. The walker's state after h steps is $|\Psi_h\rangle = \Gamma_h |\Psi_0\rangle$. Finally, the two registers are measured. Note that in the previous work generally only the first register is measured, whereas here we measure the two registers. This will double the success probability for our problems as shown later. The success probability of getting a marked vertex is

$$P_h = \sum_{u \text{ or } v \text{ is marked}} |\langle uv|\, \Gamma_h\, |\Psi_0\rangle|^2.$$

Figure 4 illustrates the success probability of finding a marked item as a function of steps in Algorithm 1 and the one with $\alpha = \beta = \pm\pi$ in Eq. (1). They show that Algorithm 1 is a robust search model.

Proof of Theorem 1. According to the arrangement of the marked vertices, two cases are discussed: they are on one side and two sides, as shown in Figs. 3(b) and 3(c), respectively.

(i) In the first case, without loss of generality, suppose that all the marked vertices lie on the left side V_l. Then, by Theorem 2, if $h \geqslant \ln(\frac{2}{\sqrt{\epsilon}})\sqrt{\frac{N_l}{n_l}} + 1$, then Algorithm 1 will output a marked vertex with probability at least $1-\epsilon$.

(ii) In the second case, by Theorem 3, if $h \geqslant \ln(\frac{2}{\sqrt{\epsilon}})\max(\sqrt{\frac{N_l}{n_l}}, \sqrt{\frac{N_r}{n_r}}) + 1$, then Algorithm 1 will output a marked vertex with probability at least $1-\epsilon^2$.

Note that the parameters α_i, β_i will be assigned with the same values in the two cases (this can be seen from the proof of Theorems 2 and 3). Thus, we need not know the arrangement of marked vertices. In addition, in the two cases, both $\sqrt{\frac{N_l}{n_l}}$ and $\max(\sqrt{\frac{N_l}{n_l}}, \sqrt{\frac{N_r}{n_r}})$ have the same upper bound $\max(\sqrt{N_l}, \sqrt{N_r})$. Therefore, if $h \geqslant \ln(\frac{2}{\sqrt{\epsilon}})\max(\sqrt{N_l}, \sqrt{N_r}) + 1$, then Algorithm 1 will output a marked vertex with probability at least $1-\epsilon$. This completes the proof.

Theorem 2. In Algorithm 1, suppose that all the marked vertices are on the left side. There exists a sequence of parameters α_i, β_i, such that if $h \geqslant \ln(\frac{2}{\sqrt{\epsilon}})\sqrt{\frac{N_l}{n_l}} + 1$, then the algorithm will output a marked vertex with probability at least $1-\epsilon$, where N_l is the number of left vertices and n_l is the total number of marked vertices.

Proof. According to Lemma 2, when h is odd, to ensure $P_h \geqslant 1-\epsilon$, it suffices to satisfy $|\cos(\frac{1}{h}\arccos(\frac{1}{\sqrt{\epsilon}}))\sqrt{1-\frac{n_l}{N_l}}| \leqslant 1$, that is,

$$\frac{n_l}{N_l} \geqslant 1 - \cos^{-2}\left[\frac{1}{h}\arccos\left(\frac{1}{\sqrt{\epsilon}}\right)\right]. \tag{5}$$

Note that the following functions (see, for instance, Ref. [42]) will be used:

$$\arccos(z) = \frac{1}{i}\ln(z + \sqrt{z^2-1}), \quad \tan(iz) = i\tanh(z),$$

$$\tanh(x) = \frac{e^x - e^{-x}}{e^x + e^{-x}},$$

where $\ln(\cdot)$ is the natural logarithm function, i denotes the imaginary number, x is a real number, and z is a complex number. Now we have

$$1 - \cos^{-2}\left[\frac{1}{h}\arccos\left(\frac{1}{\sqrt{\epsilon}}\right)\right] = -\tan^2\left[\frac{1}{h}\arccos\left(\frac{1}{\sqrt{\epsilon}}\right)\right]$$

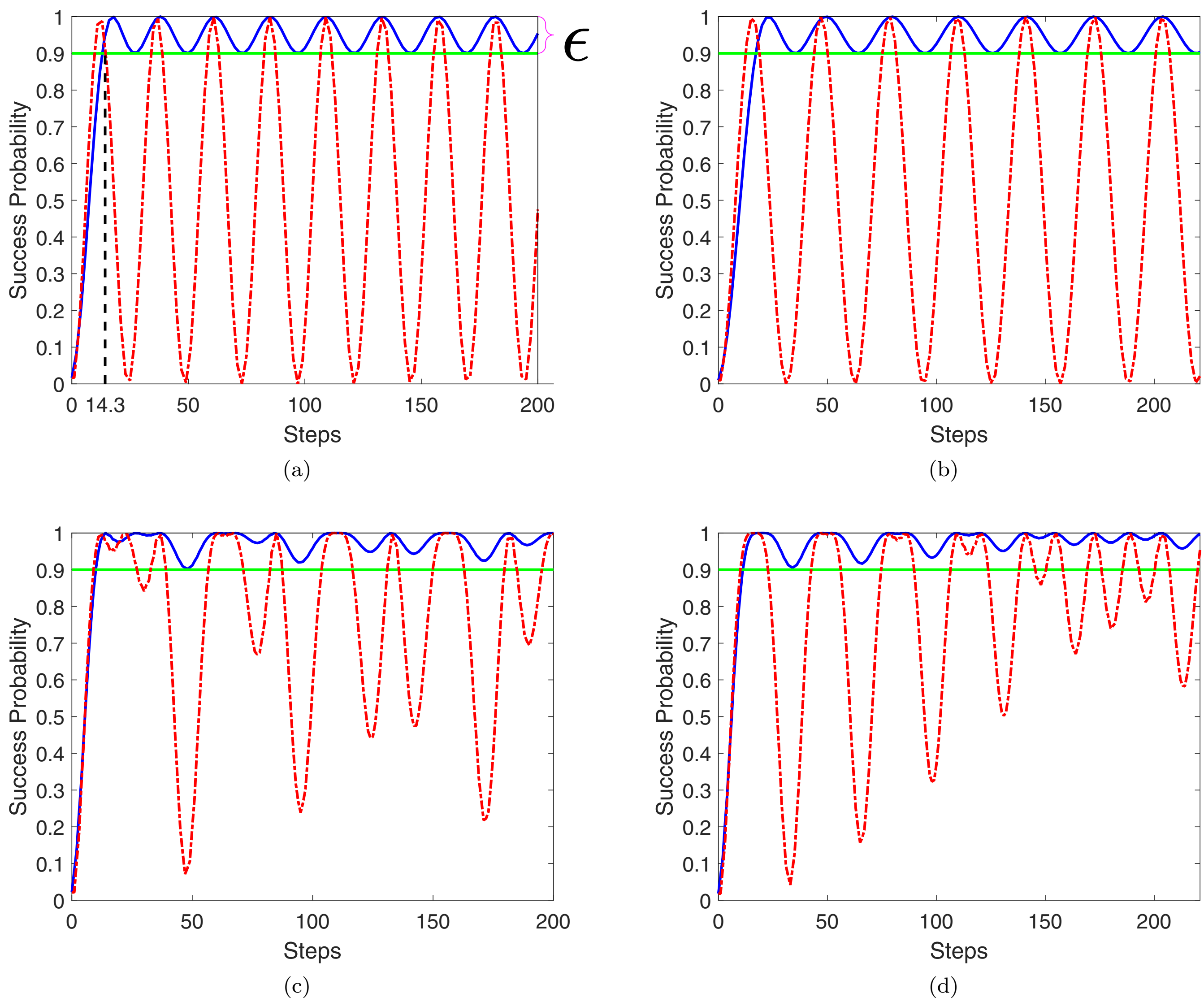

FIG. 4. The success probability of finding a marked item as a function of steps in Algorithm 1 (blue solid curve) and the one with $\alpha = \beta = \pm\pi$ in Eq. (1) (red dash-dot curve). The green horizontal solid line indicates that the success probability is greater than or equal to 0.9. (a) $N_l = 600$, $n_l = 10$, $N_r = 1000$, $n_r = 0$. The success probability $P_h \geqslant 0.9$ when $h \geqslant \ln(\frac{2}{\sqrt{\epsilon}})\sqrt{\frac{N_l}{n_l}} \approx 14.3$ with $\epsilon = 0.1$. (b) $N_l = 1000$, $n_l = 10$, $N_r = 600$, $n_r = 0$. (c) $N_l = 600$, $n_l = 10$, $N_r = 1000$, $n_r = 5$. (d) $N_l = 1000$, $n_l = 10$, $N_r = 600$, $n_r = 5$.

$$
\begin{aligned}
&= -\tan^2\left(\frac{1}{h}\frac{1}{i}\ln\left(\frac{1}{\sqrt{\epsilon}} + \sqrt{\left(\frac{1}{\sqrt{\epsilon}}\right)^2 - 1}\right)\right)\\
&= -\tan^2\left(i\frac{1}{h}\ln\left(\frac{1}{\sqrt{\epsilon}} + \sqrt{\left(\frac{1}{\sqrt{\epsilon}}\right)^2 - 1}\right)\right)\\
&= \tanh^2\left(\frac{1}{h}\ln\left(\frac{1}{\sqrt{\epsilon}} + \sqrt{\left(\frac{1}{\sqrt{\epsilon}}\right)^2 - 1}\right)\right)\\
&< \tanh^2\left[\frac{1}{h}\ln\left(\frac{2}{\sqrt{\epsilon}}\right)\right]\\
&< \left(\frac{\ln(2/\sqrt{\epsilon})}{h}\right)^2,
\end{aligned}
$$

where the last inequality follows from $x \geqslant \tanh(x)$ for $x \geqslant 0$. Thus, to ensure the inequality (5), it suffices to set $\frac{n_l}{N_l} \geqslant (\frac{\ln(2/\sqrt{\epsilon})}{h})^2$, which leads to $h \geqslant \ln(\frac{2}{\sqrt{\epsilon}})\sqrt{\frac{N_l}{n_l}}$.

Similarly, when h is even, to ensure $P_h \geqslant 1 - \epsilon$, it suffices to satisfy $|\cos(\frac{1}{h+1}\arccos(\frac{1}{\sqrt{\epsilon}}))\sqrt{1 - \frac{n_l}{N_l}}| \leqslant 1$, and $|\cos(\frac{1}{h-1}\arccos(\frac{1}{\sqrt{\epsilon}}))\sqrt{1 - \frac{n_l}{N_l}}| \leqslant 1$, which implies $h + 1 \geqslant \ln(\frac{2}{\sqrt{\epsilon}})\sqrt{\frac{N_l}{n_l}}$ and $h - 1 \geqslant \ln(\frac{2}{\sqrt{\epsilon}})\sqrt{\frac{N_l}{n_l}}$, respectively.

Thus, no matter if h is odd or even, $P_h \geqslant 1 - \epsilon$ holds for $h \geqslant \ln(\frac{2}{\sqrt{\epsilon}})\sqrt{\frac{N_l}{n_l}} + 1$. This completes the proof of Theorem 2.

Theorem 3. In Algorithm 1, suppose that the marked vertices are on both the left and right sides. There exists a sequence of parameters α_i, β_i, such that if $h \geqslant \ln(\frac{2}{\sqrt{\epsilon}})\max(\sqrt{\frac{N_l}{n_l}}, \sqrt{\frac{N_r}{n_r}}) + 1$, then the algorithm will output a marked vertex with probability at least $1-\epsilon^2$, where N_l (N_r) is the number of left (right) vertices and n_l (n_r) is the number of marked vertices on the left (right) side.

Proof. Similar to the proof of Theorem 2, by Lemma 3 one can show that:

(i) When h is odd, to ensure $P_h \geqslant 1-\epsilon^2$, it suffices to satisfy $h \geqslant \ln(\frac{2}{\sqrt{\epsilon}})\sqrt{\frac{N_l}{n_l}}$ and $h \geqslant \ln(\frac{2}{\sqrt{\epsilon}})\sqrt{\frac{N_r}{n_r}}$.

(ii) When h is even, to ensure $P_h \geqslant 1-\epsilon^2$, it suffices to satisfy $h+1 \geqslant \ln(\frac{2}{\sqrt{\epsilon}})\sqrt{\frac{N_l}{n_l}}$, $h-1 \geqslant \ln(\frac{2}{\sqrt{\epsilon}})\sqrt{\frac{N_r}{n_r}}$, $h-1 \geqslant \ln(\frac{2}{\sqrt{\epsilon}})\sqrt{\frac{N_l}{n_l}}$ and $h+1 \geqslant \ln(\frac{2}{\sqrt{\epsilon}})\sqrt{\frac{N_r}{n_r}}$.

Therefore, no matter if h is even or odd, $P_h \geqslant 1-\epsilon^2$ holds for $h \geqslant \ln(\frac{2}{\sqrt{\epsilon}})\max(\sqrt{\frac{N_l}{n_l}}, \sqrt{\frac{N_r}{n_r}})+1$. This completes the proof of Theorem 3.

Lemma 2. In Algorithm 1, suppose that all the marked vertices are on the left side. There exists a sequence of parameters α_i, β_i, such that the success probability satisfies

$$P_h = 1-\epsilon T_h^2\left(\cos\left(\frac{1}{h}\arccos\left(\frac{1}{\sqrt{\epsilon}}\right)\right)\sqrt{1-\frac{n_l}{N_l}}\right)$$

for odd h, and

$$P_h = 1-\frac{\epsilon}{2}\left(T_{h+1}^2\left(\cos\left(\frac{1}{h+1}\arccos\left(\frac{1}{\sqrt{\epsilon}}\right)\right)\sqrt{1-\frac{n_l}{N_l}}\right)\right. \\ \left. +T_{h-1}^2\left(\cos\left(\frac{1}{h-1}\arccos\left(\frac{1}{\sqrt{\epsilon}}\right)\right)\sqrt{1-\frac{n_l}{N_l}}\right)\right),$$

for even h.

Lemma 3. In Algorithm 1, suppose that the marked vertices are in both the left and right sides. There exists a sequence of parameters α_i, β_i, such that the success probability satisfies

$$P_h = 1-\epsilon^2 T_h^2\left(\cos\left(\frac{1}{h}\arccos\left(\frac{1}{\sqrt{\epsilon}}\right)\right)\sqrt{1-\frac{n_l}{N_l}}\right) \\ \times T_h^2\left(\cos\left(\frac{1}{h}\arccos\left(\frac{1}{\sqrt{\epsilon}}\right)\right)\sqrt{1-\frac{n_r}{N_r}}\right)$$

for odd h, and

$$P_h = 1-\frac{\epsilon^2}{2}\left[T_{h+1}^2\left(\cos\left(\frac{1}{h+1}\arccos\left(\frac{1}{\sqrt{\epsilon}}\right)\right)\sqrt{1-\frac{n_l}{N_l}}\right)\right. \\ \times T_{h-1}^2\left(\cos\left(\frac{1}{h-1}\arccos\left(\frac{1}{\sqrt{\epsilon}}\right)\right)\sqrt{1-\frac{n_r}{N_r}}\right) \\ + T_{h+1}^2\left(\cos\left(\frac{1}{h+1}\arccos\left(\frac{1}{\sqrt{\epsilon}}\right)\right)\sqrt{1-\frac{n_r}{N_r}}\right) \\ \left.\times T_{h-1}^2\left(\cos\left(\frac{1}{h-1}\arccos\left(\frac{1}{\sqrt{\epsilon}}\right)\right)\sqrt{1-\frac{n_l}{N_l}}\right)\right]$$

for even h.

IV. METHOD

The section is devoted to the proof of Lemma 2. As shown in Fig. 3(b), vertices can be classified into three types: the marked vertices denoted by u on the left, the unmarked vertices denoted by v on the left and s on the right. Therefore, our analysis can be simplified in a four-dimensional subspace with the orthogonal basis $\{|us\rangle, |su\rangle, |sv\rangle, |vs\rangle\}$ given below:

$$|us\rangle = \frac{1}{\sqrt{n_l}}\sum_u |u\rangle \otimes \frac{1}{\sqrt{N_r}}\sum_s |s\rangle,$$

$$|sv\rangle = \frac{1}{\sqrt{N_r}}\sum_s |s\rangle \otimes \frac{1}{\sqrt{N_L-n_l}}\sum_v |v\rangle,$$

$$|su\rangle = \frac{1}{\sqrt{N_r}}\sum_s |s\rangle \otimes \frac{1}{\sqrt{n_l}}\sum_u |u\rangle,$$

$$|vs\rangle = \frac{1}{\sqrt{N_l-n_l}}\sum_v |v\rangle \otimes \frac{1}{\sqrt{N_r}}\sum_s |s\rangle.$$

Note that $|\Psi_0\rangle$ can be rewritten in the above basis as $|\Psi_0\rangle = \frac{1}{\sqrt{2N_l N_r}}[\sqrt{n_l N_r}\,|us\rangle + \sqrt{n_l N_r}\,|su\rangle + \sqrt{N_r(N_l-n_l)}\,|sv\rangle + \sqrt{N_r(N_l-n_l)}\,|vs\rangle]$.

Hence, it can be expressed as a four-dimensional vector:

$$|\Psi_0\rangle = \frac{1}{\sqrt{2N_l N_r}}\begin{pmatrix}\sqrt{n_l N_r}\\ \sqrt{n_l N_r}\\ \sqrt{N_r(N_l-n_l)}\\ \sqrt{N_r(N_l-n_l)}\end{pmatrix}.$$

Furthermore, we have

$$S = \begin{pmatrix}0&1&0&0\\1&0&0&0\\0&0&0&1\\0&0&1&0\end{pmatrix},\quad Q(\beta) = \begin{pmatrix}e^{i\beta}&0&0&0\\0&1&0&0\\0&0&1&0\\0&0&0&1\end{pmatrix},$$

and

$$C(\alpha) = \begin{pmatrix}-e^{-i\alpha}&0&0&0\\0&C_{22}&\frac{(1-e^{-i\alpha})\sin(\omega)}{2}&0\\0&\frac{(1-e^{-i\alpha})\sin(\omega)}{2}&C_{33}&0\\0&0&0&-e^{-i\alpha}\end{pmatrix},$$

with $\omega = \arccos(1-\frac{2n_l}{N_l})$, where $C_{23} = \frac{(1-e^{-i\alpha})(1-\cos(\omega))}{2}-1$, $C_{33} = \frac{(1-e^{-i\alpha})(1+\cos(\omega))}{2}-1$, and $\cos(\omega) = 1-\frac{2n_l}{N_l}$, $\sin(\omega) = \frac{2}{N_L}\sqrt{n_l*(N_l-n_l)}$.

Now some key results are given as follows: Let

$$R(\theta) = -\begin{pmatrix}e^{-\frac{i\theta}{2}}&0&0&0\\0&e^{\frac{i\theta}{2}}&0&0\\0&0&e^{-\frac{i\theta}{2}}&0\\0&0&0&e^{-\frac{i\theta}{2}}\end{pmatrix}$$

and

$$A(\theta) = \begin{pmatrix}1&0&0&0\\0&\cos\left(\frac{\omega}{2}\right)&-ie^{i\theta}\sin\left(\frac{\omega}{2}\right)&0\\0&-ie^{-i\theta}\sin\left(\frac{\omega}{2}\right)&\cos\left(\frac{\omega}{2}\right)&0\\0&0&0&1\end{pmatrix},$$

with $\omega = \arccos(1-\frac{2n_l}{N_l})$. One can verify the following identities:

$$C(\alpha) = e^{-\frac{i\alpha}{2}}A\left(\frac{\pi}{2}\right)R(\alpha)A\left(-\frac{\pi}{2}\right), \quad (6)$$

$$Q(\beta)S = -e^{i\frac{\beta}{2}}SR(\beta), \quad (7)$$

$$A(\alpha+\beta) = R(\beta)A(\alpha)R(-\beta), \tag{8}$$
$$R(\theta)R(-\theta) = I, \tag{9}$$
$$|\Psi_0\rangle = A\left(\frac{\pi}{2}\right)SA\left(\frac{\pi}{2}\right)|\bar{0}\rangle, \tag{10}$$

where $|\bar{0}\rangle$ denotes $(0, 0, \frac{1}{\sqrt{2}}, \frac{1}{\sqrt{2}})^T$. Another crucial observation is the following lemma, which will be useful later:

Lemma 4.

$$SB_1SB_2S = B_2SB_1, \tag{11}$$

where $B_1 = \prod_{i=0}^{n} D_i$ and $B_2 = \prod_{i=0}^{m} D_i$ for $D_i \in \{A(\theta_i), R(\theta_i)\}$.

Proof. By calculation, the form of B_1 and B_2 is as follows:

$$B_1 = \begin{pmatrix} 1 & 0 & 0 & 0 \\ 0 & B_1(22) & B_1(23) & 0 \\ 0 & B_1(32) & B_1(33) & 0 \\ 0 & 0 & 0 & 1 \end{pmatrix}$$

and

$$B_2 = \begin{pmatrix} 1 & 0 & 0 & 0 \\ 0 & B_2(22) & B_2(23) & 0 \\ 0 & B_2(32) & B_2(33) & 0 \\ 0 & 0 & 0 & 1 \end{pmatrix},$$

where $B_1(\cdot)$ and $B_2(\cdot)$ are mathematical expressions of θ and ω. Hence, we have $SB_1SB_2S = B_2SB_1$.

Below we will prove Lemma 2 by two cases.

Case 1: h is an odd integer. First, we set

$$\alpha_k = \begin{cases} -\beta_{h+2-k} & k = 2, 4, \dots, h-1 \\ -\beta_{h-k} & k = 3, 5, \dots, h. \end{cases} \tag{12}$$

Then $|\Psi_h\rangle$ reduces to

$$|\Psi_h\rangle \sim S[A(\eta_h)...A(\eta_1)]R(\alpha_1)SR(\beta_h)[A(\zeta_h)...A(\zeta_1)]|\bar{0}\rangle, \tag{13}$$

which will be proven in Appendix C by using Eqs. (6)–(11). Here $\eta_k = \eta_{h+1-k}$ and $\zeta_k = \zeta_{h+1-k}$ for $k = 1, 2, \dots, h$, and

$$\eta_{k+1} - \eta_k = \begin{cases} \pi - \alpha_{k+1} & k = 2, 4, \dots, h-1 \\ -\pi + \alpha_{h-k+1} & k = 3, 5, \dots, h, \end{cases} \tag{14}$$
$$\zeta_{k+1} - \zeta_k = \begin{cases} \pi - \alpha_k & k = 2, 4, \dots, h-1 \\ -\pi + \alpha_{h-k} & k = 3, 5, \dots, h. \end{cases} \tag{15}$$

Let us have a more detailed analysis at the state evolution in Eq. (13), which can be divided into four stages as follows:

$$\frac{1}{\sqrt{2}}\begin{pmatrix} 0 \\ 0 \\ 1 \\ 1 \end{pmatrix} \xrightarrow[\text{①}]{A(\zeta_h)...A(\zeta_1)} \frac{1}{\sqrt{2}}\begin{pmatrix} 0 \\ b_h(x) \\ c_h(x) \\ 1 \end{pmatrix}$$
$$\xrightarrow[\text{②}]{R(\alpha_1)SR(\beta_h)} \frac{1}{\sqrt{2}}\begin{pmatrix} e^{i\beta_h}b_h(x) \\ 0 \\ 1 \\ c_h(x) \end{pmatrix}$$
$$\xrightarrow[\text{③}]{A(\eta_h)...A(\eta_1)} \frac{1}{\sqrt{2}}\begin{pmatrix} e^{i\beta_h}b_h(x) \\ \bar{b}_h(x) \\ \bar{c}_h(x) \\ c_h(x) \end{pmatrix}$$
$$\xrightarrow[\text{④}]{S} \frac{1}{\sqrt{2}}\begin{pmatrix} \bar{b}_h(x) \\ e^{i\beta_h}b_h(x) \\ c_h(x) \\ \bar{c}_h(x) \end{pmatrix}.$$

Stage ①: Apply $A(\zeta_h)...A(\zeta_1)$ to the initial state. Let $(a_0, b_0, c_0, d_0) = (0, 0, 1, 1)$ and

$$|\mu_k\rangle = \begin{pmatrix} a_k \\ b_k \\ c_k \\ d_k \end{pmatrix} = A(\zeta_k)...A(\zeta_1)\begin{pmatrix} 0 \\ 0 \\ 1 \\ 1 \end{pmatrix}$$

for $k = 1, 2, \dots, h$. First note that $A(\zeta_i)$ has an effect only on the second and third dimensions of a four-dimensional vector. Thus, $a_k = 0$ and $d_k = 1$ for all k. Furthermore, we have

$$\begin{aligned} |\mu_k\rangle &= A(\zeta_k)|\mu_{k-1}\rangle \\ &= \begin{pmatrix} 0 \\ b_{k-1}\cos\left(\frac{\omega}{2}\right) - ic_{k-1}e^{i\zeta_k}\sin\left(\frac{\omega}{2}\right) \\ -ib_{k-1}e^{-i\zeta_k}\sin\left(\frac{\omega}{2}\right) + c_{k-1}\cos\left(\frac{\omega}{2}\right) \\ 1 \end{pmatrix} \end{aligned} \tag{16}$$

and

$$\begin{aligned} |\mu_{k-2}\rangle &= A(\zeta_{k-1})^{-1}|\mu_{k-1}\rangle \\ &= \begin{pmatrix} 0 \\ b_{k-1}\cos\left(\frac{\omega}{2}\right) + ic_{k-1}e^{i\zeta_{k-1}}\sin\left(\frac{\omega}{2}\right) \\ ib_{k-1}e^{-i\zeta_{k-1}}\sin\left(\frac{\omega}{2}\right) + c_{k-1}\cos\left(\frac{\omega}{2}\right) \\ 1 \end{pmatrix}. \end{aligned} \tag{17}$$

Combined with Eqs. (16) and (17), we have

$$c_k = -ib_{k-1}e^{-i\zeta_k}\sin\left(\frac{\omega}{2}\right) + c_{k-1}\cos\left(\frac{\omega}{2}\right),$$
$$c_{k-2} = ib_{k-1}e^{-i\zeta_{k-1}}\sin\left(\frac{\omega}{2}\right) + c_{k-1}\cos\left(\frac{\omega}{2}\right).$$

The recurrence formula of $c_k(x)$ is defined by $c_0(x) = 1$, $c_1(x) = x$, and for $k = 2, \dots, h$,

$$c_k(x) = x(1 + e^{-i(\zeta_k - \zeta_{k-1})})c_{k-1}(x) - e^{-i(\zeta_k - \zeta_{k-1})}c_{k-2}(x),$$

with $x = \cos(\frac{\omega}{2})$. By Lemma 1, when

$$\zeta_{k+1} - \zeta_k = (-1)^k\pi - 2\text{arccot}\left[\tan\left(\frac{k\pi}{h}\right)\sqrt{1-\gamma^2}\right] \tag{18}$$

for $k = 1, \dots, h-1$, where $\gamma^{-1} = \cos[\frac{1}{h}\arccos(\frac{1}{\sqrt{\epsilon}})]$, we have

$$c_h(x) = \frac{T_h\left(\frac{x}{\gamma}\right)}{T_h\left(\frac{1}{\gamma}\right)},$$

with $T_h(\frac{1}{\gamma}) = \frac{1}{\sqrt{\epsilon}}$. Moreover, $b_h(x)$ is determined by $|b_h(x)|^2 + |c_h(x)|^2 = 1$. Therefore, the state after $A(\zeta_h)...A(\zeta_1)$ applied to the initial state is

$$\frac{1}{\sqrt{2}}\begin{pmatrix} 0 \\ b_h(x) \\ c_h(x) \\ 1 \end{pmatrix}.$$

Stage ②: Apply $R(\alpha_1)SR(\beta_h)$ to the above state. After that, the state is

$$\frac{1}{\sqrt{2}}\begin{pmatrix} e^{i\beta_h}b_h(x) \\ 0 \\ 1 \\ c_h(x) \end{pmatrix}.$$

Stage ③: Perform $A(\eta_h)...A(\eta_1)$. Let

$$\begin{pmatrix} \bar{a}_k \\ \bar{b}_k \\ \bar{c}_k \\ \bar{d}_k \end{pmatrix} = A(\eta_k)...A(\eta_1)\begin{pmatrix} e^{i\beta_h}b_h(x) \\ 0 \\ 1 \\ c_h(x) \end{pmatrix}$$

for $k = 1, 2, \dots, h$. By the property of the matrix $A(\eta_i)$, we have $\bar{a}_k = e^{i\beta_h}b_h(x)$ and $\bar{d}_k = c_h(x)$ for all k. The recurrence formula of $\bar{c}_k(x)$ is defined by $\bar{c}_0(x) = 1$, $\bar{c}_1(x) = x$ and for $k = 2, \dots, h$,

$$\bar{c}_k(x) = x(1 + e^{-i(\eta_k-\eta_{k-1})})\bar{c}_{k-1}(x) - e^{-i(\eta_k-\eta_{k-1})}\bar{c}_{k-2}(x),$$

with $x = \cos(\frac{\omega}{2})$. By Lemma 1, when

$$\eta_{k+1} - \eta_k = (-1)^k\pi - 2\cot^{-1}\left(\tan\left(\frac{k\pi}{h}\right)\sqrt{1-\gamma^2}\right) \quad (19)$$

for $k = 1, \dots, h-1$, where $\gamma^{-1} = \cos(\frac{1}{h}\arccos(\frac{1}{\sqrt{\epsilon}}))$, we have

$$\bar{c}_h(x) = \frac{T_h\left(\frac{x}{\gamma}\right)}{T_h\left(\frac{1}{\gamma}\right)},$$

with $T_h(\frac{1}{\gamma}) = \frac{1}{\sqrt{\epsilon}}$. Moreover, $\bar{b}_h(x)$ is determined by $|\bar{b}_h(x)|^2 + |\bar{c}_h(x)|^2 = 1$. Hence, the result state is

$$\frac{1}{\sqrt{2}}\begin{pmatrix} e^{i\beta_h}b_h(x) \\ \bar{b}_h(x) \\ \bar{c}_h(x) \\ c_h(x) \end{pmatrix}.$$

Stage ④: Perform the final operation S. The final state is

$$\frac{1}{\sqrt{2}}\begin{pmatrix} \bar{b}_h(x) \\ e^{i\beta_h}b_h(x) \\ c_h(x) \\ \bar{c}_h(x) \end{pmatrix}.$$

Therefore, the success probability P_h is

$$P_h = 1 - \frac{1}{2}(|c_h(x)|^2 + |\bar{c}_h(x)|^2) = 1 - \epsilon T_h^2\left(\frac{x}{\gamma}\right)$$
$$= 1 - \epsilon T_h^2\left(\cos\left(\frac{1}{h}\arccos\left(\frac{1}{\sqrt{\epsilon}}\right)\right)\sqrt{1-\frac{n_l}{N_l}}\right).$$

By Eqs. (12), (14), (15), (18), and (19), α_k, β_k can be chosen such that

$$\alpha_k = -\beta_{h+2-k} = \pi + (\eta_{k+1} - \eta_k)$$
$$= 2\text{arccot}\left[\tan\left(\frac{k\pi}{h}\right)\sqrt{1-\gamma^2}\right]$$

for $k = 2, 4, \dots, h-1$, and

$$\alpha_k = -\beta_{h-k} = \pi - (\zeta_{k+1} - \zeta_k)$$
$$= 2\text{arccot}\left[\tan\left(\frac{(k-1)\pi}{h}\right)\sqrt{1-\gamma^2}\right]$$

for $k = 3, 5, \dots, h$. In addition, α_1 and β_h can be any value.

Case 2: h is an even integer. The proof is given in Appendix A.

V. CONCLUSION AND OUTLOOK

In this paper, we investigated how to overcome the soufflé problem of quantum walk search. We presented a robust quantum walk-based algorithm for searching a marked vertex on a complete bipartite graph. The algorithm need not know any prior information about the marked vertices (e.g., the number of marked vertices) but keeps a quadratic speedup over classical search algorithms and ensures that the error is bounded by a tunable parameter ϵ.

We have just initiated a step toward robust quantum walk search. More questions are worthy of further consideration. For example, several interesting questions are listed below:

(i) Can the robustness feature be introduced into quantum walk search on other graphs?

(ii) For the framework of searching a marked state in Markov chains, can we propose a robust version?

(iii) Another interesting direction would be to explore some important problems in practical scenarios by robust quantum walk search algorithms.

We will try to address these questions in forthcoming works.

ACKNOWLEDGMENTS

This work was supported by the National Natural Science Foundation of China (Grants No. 62272492 and No. 61772565) and the Guangdong Basic and Applied Basic Research Foundation (Grant No. 2020B1515020050).

APPENDIX A: CASE 2 IN THE PROOF OF LEMMA 2: *h* IS AN EVEN INTEGER

First, we set

$$\beta_k = -\alpha_{h+1-k} \quad k = 1, 2, \dots, h-1. \quad (A1)$$

Then $|\Psi_h\rangle$ reduces to

$$|\Psi_h\rangle \sim R(\beta_h)[A(\phi_{h-1})...A(\phi_1)]R(\alpha_1)S[A(\psi_{h+1})...A(\psi_1)]\,|\bar{0}\rangle\,, \quad (A2)$$

which will be proven in Appendix C by using Eqs. (6)–(11). Here $\phi_k = \phi_{h-k}$ for $k = 1, 2, \dots, h-1$, $\psi_k = \psi_{h+2-k}$ for $k = 1, 2, \dots, h+1$, and

$$\phi_{k+1} - \phi_k = \begin{cases} \pi - \alpha_{k+1} & k = 2, 4, \dots, h-2 \\ -\pi + \alpha_{h-k} & k = 1, 3, \dots, h-3, \end{cases} \tag{A3}$$

$$\psi_{k+1} - \psi_k = \begin{cases} \pi - \alpha_k & k = 2, 4, \dots, h-2 \\ -\pi + \alpha_{h-k+1} & k = 1, 3, \dots, h. \end{cases} \tag{A4}$$

Similar to Eq. (13), the final state of Eq. (A2) can be obtained by the following four stages:

$$\frac{1}{\sqrt{2}}\begin{pmatrix}0\\0\\1\\1\end{pmatrix} \xrightarrow[\text{①}]{A(\psi_{h+1})\dots A(\psi_1)} \frac{1}{\sqrt{2}}\begin{pmatrix}0\\b_{h+1}(x)\\c_{h+1}(x)\\1\end{pmatrix} \xrightarrow[\text{②}]{R(\alpha_1)S} \frac{1}{\sqrt{2}}\begin{pmatrix}b_{h+1}(x)\\0\\1\\c_{h+1}(x)\end{pmatrix} \xrightarrow[\text{③}]{A(\phi_{h-1})\dots A(\phi_1)} \frac{1}{\sqrt{2}}\begin{pmatrix}b_{h+1}(x)\\\bar{b}_{h-1}(x)\\\bar{c}_{h-1}(x)\\c_{h+1}(x)\end{pmatrix} \xrightarrow[\text{④}]{R(\beta_h)} \frac{1}{\sqrt{2}}\begin{pmatrix}b_{h+1}(x)\\e^{i\beta_h}\bar{b}_{h-1}(x)\\\bar{c}_{h-1}(x)\\c_{h+1}(x)\end{pmatrix}.$$

Stage ①: Apply $A(\psi_{h+1})\dots A(\psi_1)$ to the initial state. Let $(a_0, b_0, c_0, d_0) = (0, 0, 1, 1)$ and

$$\begin{pmatrix}a_k\\b_k\\c_k\\d_k\end{pmatrix} = A(\psi_k)\dots A(\psi_1)\begin{pmatrix}0\\0\\1\\1\end{pmatrix}$$

for $k = 1, 2, \dots, h+1$. By the property of matrix $A(\psi_i)$, we have $a_k = 0$ and $d_k = 1$ for all k. The recurrence formula of $c_k(x)$ is defined by $c_0(x) = 1$, $c_1(x) = x$ and for $k = 2, \dots, h+1$,

$$c_k(x) = x(1 + e^{-i(\psi_k - \psi_{k-1})})c_{k-1}(x) - e^{-i(\psi_k - \psi_{k-1})}c_{k-2}(x),$$

with $x = \cos(\frac{\omega}{2})$. By Lemma 1, when

$$\psi_{k+1} - \psi_k = (-1)^k\pi - 2\mathrm{arccot}\left(\tan\left(\frac{k\pi}{h+1}\right)\sqrt{1-\gamma_1^2}\right), \tag{A5}$$

with $\gamma_1^{-1} = \cos(\frac{1}{h+1}\arccos(\frac{1}{\sqrt{\epsilon}}))$ for $k = 1, 2, \dots, h$, we have

$$c_{h+1}(x) = \frac{T_{h+1}(\frac{x}{\gamma_1})}{T_{h+1}(\frac{1}{\gamma_1})},$$

with $T_{h+1}(\frac{1}{\gamma_1}) = \frac{1}{\sqrt{\epsilon}}$. Moreover, $b_{h+1}(x)$ is determined by $|b_{h+1}(x)|^2 + |c_{h+1}(x)|^2 = 1$. Therefore, the state after $A(\psi_{h+1})\dots A(\psi_1)$ applied to the initial state is

$$\frac{1}{\sqrt{2}}\begin{pmatrix}0\\b_{h+1}(x)\\c_{h+1}(x)\\1\end{pmatrix}.$$

Stage ②: Apply $R(\alpha_1)S$ to the above state. After that, the state is

$$\frac{1}{\sqrt{2}}\begin{pmatrix}b_{h+1}(x)\\0\\1\\c_{h+1}(x)\end{pmatrix}.$$

Stage ③: Perform $A(\phi_{h-1})\dots A(\phi_1)$. Let

$$\begin{pmatrix}\bar{a}_k\\\bar{b}_k\\\bar{c}_k\\\bar{d}_k\end{pmatrix} = A(\phi_k)\dots A(\phi_1)\begin{pmatrix}b_{h+1}(x)\\0\\1\\c_{h+1}(x)\end{pmatrix}$$

for $k = 1, 2, \dots, h-1$. By the property of matrix $A(\phi_i)$, we have $\bar{a}_k = b_{h+1}(x)$ and $\bar{d}_k = c_{h+1}(x)$ for all k. The recurrence formula of $\bar{c}_k(x)$ is defined by $\bar{c}_0(x) = 1$, $\bar{c}_1(x) = x$ and for $k = 2, \dots, h-1$,

$$\bar{c}_k(x) = x(1 + e^{-i(\phi_k - \phi_{k-1})})\bar{c}_{k-1}(x) - e^{-i(\phi_k - \phi_{k-1})}\bar{c}_{k-2}(x),$$

with $x = \cos(\frac{\omega}{2})$. By Lemma 1, when

$$\phi_{k+1} - \phi_k = (-1)^k\pi - 2\mathrm{arccot}\left(\tan\left(\frac{k\pi}{h-1}\right)\sqrt{1-\gamma_2^2}\right), \tag{A6}$$

with $\gamma_2^{-1} = \cos[\frac{1}{h-1}\arccos(\frac{1}{\sqrt{\epsilon}})]$ for $k = 1, 2, \ldots, h-2$, we have

$$\bar{c}_{h-1}(x) = \frac{T_{h-1}\left(\frac{x}{\gamma_2}\right)}{T_{h-1}\left(\frac{1}{\gamma_2}\right)},$$

with $T_{h-1}(\frac{1}{\gamma_2}) = \frac{1}{\sqrt{\epsilon}}$. Moreover, $\bar{b}_{h-1}(x)$ is determined by $|\bar{b}_{h-1}(x)|^2 + |\bar{c}_{h-1}(x)|^2 = 1$. Hence, the result state is

$$\frac{1}{\sqrt{2}}\begin{pmatrix} b_{h+1}(x) \\ \bar{b}_{h-1}(x) \\ \bar{c}_{h-1}(x) \\ c_{h+1}(x) \end{pmatrix}.$$

Stage ④: Perform the final operation $R(\beta_h)$. The final state is

$$\frac{1}{\sqrt{2}}\begin{pmatrix} b_{h+1}(x) \\ e^{i\beta_h}\bar{b}_{h-1}(x) \\ \bar{c}_{h-1}(x) \\ c_{h+1}(x) \end{pmatrix}.$$

Therefore, the success probability P_h is

$$\begin{aligned} P_h &= 1 - \frac{1}{2}(|\bar{c}_{h-1}(x)|^2 + |c_{h-1}(x)|^2) \\ &= 1 - \frac{\epsilon}{2}\left(T_{h+1}^2\left(\frac{x}{\gamma_1}\right) + T_{h-1}^2\left(\frac{x}{\gamma_2}\right)\right) \\ &= 1 - \frac{\epsilon}{2}\left[T_{h+1}^2\left(\cos\left(\frac{1}{h+1}\arccos\left(\frac{1}{\sqrt{\epsilon}}\right)\right)\sqrt{1-\frac{n_l}{N_l}}\right) + T_{h-1}^2\left(\cos\left(\frac{1}{h-1}\arccos\left(\frac{1}{\sqrt{\epsilon}}\right)\right)\sqrt{1-\frac{n_l}{N_l}}\right)\right]. \end{aligned}$$

By Eq. (A1) and Eqs. (A3)–(A6), α_k, β_k can be chosen such that

$$\alpha_k = -\beta_{h+1-k} = \pi - (\phi_k - \phi_{k-1}) = 2\text{arccot}\left(\tan\left(\frac{k\pi}{h+1}\right)\sqrt{1-\gamma_1^2}\right)$$

for $k = 2, 4, \ldots, h$, and

$$\alpha_k = -\beta_{h+1-k} = \pi - (\psi_{k+1} - \psi_k) = 2\text{arccot}\left(\tan\left(\frac{(k-1)\pi}{h-1}\right)\sqrt{1-\gamma_2^2}\right)$$

for $k = 3, 5, \ldots, h-1$. In addition, α_1 and β_h can be any value.

APPENDIX B: PROOF OF LEMMA 3: MARKED VERTICES IN TWO SIDES

The section is devoted to the proof of Lemma 3.

Proof. Vertices in Fig. 3(c) can be divided into four types: the marked vertices denoted by u on the left and t on the right, the unmarked vertices denoted by v on the left and s on the right. Hence, our analysis can be simplified in an eight-dimensional subspace defined by the following orthogonal basis $\{|ut\rangle, |us\rangle, |tu\rangle, |tv\rangle, |vt\rangle, |vs\rangle, |su\rangle, |sv\rangle\}$:

$$|ut\rangle = \frac{1}{\sqrt{n_l}}\sum_u |u\rangle \otimes \frac{1}{\sqrt{n_r}}\sum_t |t\rangle, \quad |us\rangle = \frac{1}{\sqrt{n_l}}\sum_u |u\rangle \otimes \frac{1}{\sqrt{N_r - n_r}}\sum_s |s\rangle,$$

$$|tu\rangle = \frac{1}{\sqrt{n_r}}\sum_t |t\rangle \otimes \frac{1}{\sqrt{n_l}}\sum_u |u\rangle, \quad |tv\rangle = \frac{1}{\sqrt{n_r}}\sum_t |t\rangle \otimes \frac{1}{\sqrt{N_l - n_l}}\sum_v |v\rangle,$$

$$|vt\rangle = \frac{1}{\sqrt{N_l - n_l}}\sum_v |v\rangle \otimes \frac{1}{\sqrt{n_r}}\sum_t |t\rangle,$$

$$|vs\rangle = \frac{1}{\sqrt{N_l - n_l}}\sum_v |v\rangle \otimes \frac{1}{\sqrt{N_r - n_r}}\sum_s |s\rangle,$$

$$|su\rangle = \frac{1}{\sqrt{N_r - n_r}}\sum_s |s\rangle \otimes \frac{1}{\sqrt{n_l}}\sum_u |u\rangle,$$

$$|sv\rangle = \frac{1}{\sqrt{N_r - n_r}}\sum_s |s\rangle \otimes \frac{1}{\sqrt{N_l - n_l}}\sum_v |v\rangle.$$

Then $|\Psi_0\rangle$ can be rewritten in the above basis as

$$\begin{aligned}|\Psi_0\rangle = \frac{1}{\sqrt{2N_lN_r}}[&\sqrt{n_ln_r}\,|ut\rangle + \sqrt{n_l(N_r-n_r)}\,|us\rangle + \sqrt{n_ln_r}\,|tu\rangle \\ &+ \sqrt{n_r(N_l-n_l)}\,|tv\rangle + \sqrt{n_r(N_l-n_l)}\,|vt\rangle + \sqrt{(N_l-n_l)(N_r-n_r)}\,|vs\rangle \\ &+ \sqrt{n_l(N_r-n_r)}\,|su\rangle + \sqrt{(N_l-n_l)(N_r-n_r)}\,|sv\rangle].\end{aligned}$$

Thus, $|\Psi_0\rangle$ can be expressed as an eight-dimensional vector:

$$|\Psi_0\rangle = \frac{1}{\sqrt{2N_lN_r}}\begin{pmatrix}\sqrt{n_ln_r}\\ \sqrt{n_l(N_r-n_r)}\\ \sqrt{n_ln_r}\\ \sqrt{n_r(N_l-n_l)}\\ \sqrt{n_r(N_l-n_l)}\\ \sqrt{(N_l-n_l)(N_r-n_r)}\\ \sqrt{n_l(N_r-n_r)}\\ \sqrt{(N_l-n_l)(N_r-n_r)}\end{pmatrix}.$$

Furthermore, we have

$$S = \begin{pmatrix}0&0&1&0&0&0&0&0\\0&0&0&0&0&0&1&0\\1&0&0&0&0&0&0&0\\0&0&0&0&1&0&0&0\\0&0&0&1&0&0&0&0\\0&0&0&0&0&0&0&1\\0&1&0&0&0&0&0&0\\0&0&0&0&0&1&0&0\end{pmatrix},\quad Q(\beta) = \begin{pmatrix}e^{i\beta}&0&0&0&0&0&0&0\\0&e^{i\beta}&0&0&0&0&0&0\\0&0&e^{i\beta}&0&0&0&0&0\\0&0&0&e^{i\beta}&0&0&0&0\\0&0&0&0&1&0&0&0\\0&0&0&0&0&1&0&0\\0&0&0&0&0&0&1&0\\0&0&0&0&0&0&0&1\end{pmatrix}$$

and

$$C(\alpha) = \begin{pmatrix}1&0\\0&1\end{pmatrix}\otimes\begin{pmatrix}M_1&M_2&0&0\\M_2&M_3&0&0\\0&0&M_4&M_5\\0&0&M_5&M_6\end{pmatrix},$$

with

$$\begin{aligned}M_1 &= \frac{(1-e^{-i\alpha})(1-\cos(\omega_2))}{2}-1,\quad M_2 = \frac{(1-e^{-i\alpha})\sin(\omega_2)}{2},\\ M_3 &= \frac{(1-e^{-i\alpha})(1+\cos(\omega_2))}{2}-1,\quad M_4 = \frac{(1-e^{-i\alpha})(1-\cos(\omega_1))}{2}-1,\\ M_5 &= \frac{(1-e^{-i\alpha})\sin(\omega_1)}{2},\quad M_6 = \frac{(1-e^{-i\alpha})(1+\cos(\omega_1))}{2}-1,\end{aligned}$$

where $\cos(\omega_1) = 1-\frac{2n_l}{N_l}$, $\sin(\omega_1) = \frac{2}{N_l}\sqrt{n_l(N_l-n_l)}$, $\cos(\omega_2) = 1-\frac{2n_r}{N_r}$, and $\sin(\omega_2) = \frac{2}{N_r}\sqrt{n_r(N_r-n_r)}$.

Let

$$R(\theta) = -\begin{pmatrix}e^{\frac{i\theta}{2}}&0&0&0&0&0&0&0\\0&e^{-\frac{i\theta}{2}}&0&0&0&0&0&0\\0&0&e^{\frac{i\theta}{2}}&0&0&0&0&0\\0&0&0&e^{-\frac{i\theta}{2}}&0&0&0&0\\0&0&0&0&e^{\frac{i\theta}{2}}&0&0&0\\0&0&0&0&0&e^{-\frac{i\theta}{2}}&0&0\\0&0&0&0&0&0&e^{\frac{i\theta}{2}}&0\\0&0&0&0&0&0&0&e^{-\frac{i\theta}{2}}\end{pmatrix}$$

and

$$A(\theta) = \begin{pmatrix}1&0\\0&1\end{pmatrix}\otimes\begin{pmatrix}\cos\left(\frac{\omega_2}{2}\right)&-ie^{i\theta}\frac{\sin(\omega_2)}{2}&0&0\\-ie^{-i\theta}\frac{\sin(\omega_2)}{2}&\cos\left(\frac{\omega_2}{2}\right)&0&0\\0&0&\cos\left(\frac{\omega_1}{2}\right)&-ie^{i\theta}\frac{\sin(\omega_1)}{2}\\0&0&-ie^{-i\theta}\frac{\sin(\omega_1)}{2}&\cos\left(\frac{\omega_1}{2}\right)\end{pmatrix}.$$

We have

$$C(\alpha) = e^{-\frac{i\alpha}{2}} A\left(\frac{\pi}{2}\right) R(\alpha) A\left(-\frac{\pi}{2}\right), \tag{B1}$$

$$Q(\beta)S = -e^{i\frac{\beta}{2}} SR(\beta), \tag{B2}$$

$$A(\alpha + \beta) = R(\beta)A(\alpha)R(-\beta), \tag{B3}$$

$$R(\theta)R(-\theta) = I, \tag{B4}$$

$$|\Psi_0\rangle = A\left(\frac{\pi}{2}\right) SA\left(\frac{\pi}{2}\right) |\bar{0}\rangle , \tag{B5}$$

where $|\bar{0}\rangle$ denotes $(0, 0, 0, 0, 0, \frac{1}{\sqrt{2}}, 0, \frac{1}{\sqrt{2}})^T$. Similarly to Eq. (11), the following equation holds:

$$SB_1SB_2S = B_2SB_1, \tag{B6}$$

where $B_1 = \prod_{i=0}^{n} D_i$ and $B_2 = \prod_{i=0}^{m} D_i$ for $D_i \in \{A(\theta_i), R(\theta_i)\}$.

Below we will prove Lemma 3 by two cases.

1. Case 1: *h* is an odd integer

First, we set

$$\alpha_k = \begin{cases} -\beta_{h+2-k} & k = 2, 4, \ldots, h-1 \\ -\beta_{h-k} & k = 3, 5, \ldots, h. \end{cases} \tag{B7}$$

Then $|\Psi_h\rangle$ reduces to

$$|\Psi_h\rangle \sim S[A(\eta_h)...A(\eta_1)]R(\alpha_1)SR(\beta_h)[A(\zeta_h)...A(\zeta_1)] |\bar{0}\rangle , \tag{B8}$$

which will be proven in Appendix D by using Eqs. (B1)–(B6). Here $\eta_k = \eta_{h+1-k}$, $\zeta_k = \zeta_{h+1-k}$ for $k = 1, 2, \ldots, h$, and

$$\eta_{k+1} - \eta_k = \begin{cases} \pi - \alpha_{k+1} & k = 2, 4, \ldots, h-1 \\ -\pi + \alpha_{h-k+1} & k = 3, 5, \ldots, h, \end{cases} \tag{B9}$$

$$\zeta_{k+1} - \zeta_k = \begin{cases} \pi - \alpha_k & k = 2, 4, \ldots, h-1 \\ -\pi + \alpha_{h-k} & k = 3, 5, \ldots, h. \end{cases} \tag{B10}$$

The final state of Eq. (B8) can be obtained by the following four stages:

$$\frac{1}{\sqrt{2}}\begin{pmatrix}0\\0\\0\\0\\0\\1\\0\\1\end{pmatrix} \xrightarrow[①]{A(\zeta_h)...A(\zeta_1)} \frac{1}{\sqrt{2}}\begin{pmatrix}0\\0\\0\\0\\e_h(x_2)\\f_h(x_2)\\g_h(x_1)\\l_h(x_1)\end{pmatrix} \xrightarrow[②]{R(\alpha_1)SR(\beta_h)} \frac{1}{\sqrt{2}}\begin{pmatrix}0\\e^{i\beta_h}g_h(x_1)\\0\\e^{i\beta_h}e_h(x_2)\\0\\g_h(x_1)\\0\\f_h(x_2)\end{pmatrix}$$

$$\xrightarrow[③]{A(\eta_h)...A(\eta_1)} \frac{1}{\sqrt{2}}\begin{pmatrix}e^{i\beta_h}g_h(x_1)\bar{a}_h(x_2)\\e^{i\beta_h}g_h(x_1)\bar{b}_h(x_2)\\e^{i\beta_h}e_h(x_2)\bar{c}_h(x_1)\\e^{i\beta_h}e_h(x_2)\bar{d}_h(x_1)\\g_h(x_1)\bar{e}_h(x_2)\\g_h(x_1)\bar{f}_h(x_2)\\f_h(x_2)\bar{g}_h(x_1)\\f_h(x_2)\bar{l}_h(x_1)\end{pmatrix} \xrightarrow[④]{S} \frac{1}{\sqrt{2}}\begin{pmatrix}e^{i\beta_h}e_h(x_2)\bar{c}_h(x_1)\\f_h(x_2)\bar{g}_h(x_1)\\e^{i\beta_h}g_h(x_1)\bar{a}_h(x_2)\\g_h(x_1)\bar{e}_h(x_2)\\e^{i\beta_h}e_h(x_2)\bar{d}_h(x_1)\\f_h(x_2)\bar{l}_h(x_1)\\e^{i\beta_h}g_h(x_1)\bar{b}_h(x_2)\\g_h(x_1)\bar{f}_h(x_2)\end{pmatrix}.$$

Stage ①: apply $A(\zeta_h)...A(\zeta_1)$ to the initial state. Let

$$(a_0, b_0, c_0, d_0, e_0, f_0, g_0, l_0) = (0, 0, 0, 0, 0, 1, 0, 1)$$

and

$$\begin{pmatrix} a_k \\ b_k \\ c_k \\ d_k \\ e_k \\ f_k \\ g_k \\ l_k \end{pmatrix} = A(\zeta_k)...A(\zeta_1)\begin{pmatrix} 0 \\ 0 \\ 0 \\ 0 \\ 0 \\ 1 \\ 0 \\ 1 \end{pmatrix}$$

for $k = 1, 2, \dots, h$. The elements of an eight-dimensional vector are divided into four groups: (first, second), (third, fourth), (fifth, sixth), and (seventh, eighth). Note that each block of matrix $A(\zeta_i)$ acts on a corresponding group of an eight-dimensional vector. Thus, $a_k = b_k = c_k = d_k = 0$ for all k. The recurrence formula of $l_k(x_1)$ is defined by $l_0(x_1) = 1$, $l_1(x_1) = x_1$ and for $k = 2, \dots, h$,

$$l_k(x_1) = x_1(1 + e^{-i(\zeta_k-\zeta_{k-1})})l_{k-1}(x_1) - e^{-i(\zeta_k-\zeta_{k-1})}l_{k-2}(x_1),$$

with $x_1 = \cos(\frac{\omega_1}{2})$. The recurrence formula of $f_k(x_2)$ is defined by $f_0(x_2) = 1$, $f_1(x_2) = x_2$ and for $k = 2, \dots, h$,

$$f_k(x_2) = x_2(1 + e^{-i(\zeta_k-\zeta_{k-1})})f_{k-1}(x_2) - e^{-i(\zeta_k-\zeta_{k-1})}f_{k-2}(x_2),$$

with $x_2 = \cos(\frac{\omega_2}{2})$. By Lemma 1, when

$$\zeta_{k+1} - \zeta_k = (-1)^k\pi - 2\text{arccot}\left(\tan\left(\frac{k\pi}{h}\right)\sqrt{1-\gamma^2}\right), \tag{B11}$$

with $\gamma^{-1} = \cos[\frac{1}{h}\arccos(\frac{1}{\sqrt{\epsilon}})]$ for $k = 1, 2, \dots, h-1$, we have

$$l_h(x_1) = \frac{T_h\left(\frac{x_1}{\gamma}\right)}{T_h\left(\frac{1}{\gamma}\right)}, \quad f_h(x_2) = \frac{T_h\left(\frac{x_2}{\gamma}\right)}{T_h\left(\frac{1}{\gamma}\right)},$$

with $T_h(\frac{1}{\gamma}) = \frac{1}{\sqrt{\epsilon}}$. Moreover, $e_h(x_2)$ and $g_h(x_1)$ are determined by $|e_h(x_2)|^2 + |f_h(x_2)|^2 = 1$ and $|g_h(x_1)|^2 + |l_h(x_1)|^2 = 1$, respectively. Therefore, the state after $A(\zeta_h)...A(\zeta_1)$ applied to the initial state is

$$\frac{1}{\sqrt{2}}\begin{pmatrix} 0 \\ 0 \\ 0 \\ 0 \\ e_h(x_2) \\ f_h(x_2) \\ g_h(x_1) \\ l_h(x_1) \end{pmatrix}.$$

Stage ②: Apply $R(\alpha_1)SR(\beta_h)$ to the above state. After that, the state is

$$\frac{1}{\sqrt{2}}\begin{pmatrix} 0 \\ e^{i\beta_h}g_h(x_1) \\ 0 \\ e^{i\beta_h}e_h(x_2) \\ 0 \\ g_h(x_1) \\ 0 \\ f_h(x_2) \end{pmatrix}.$$

Stage ③: Perform $A(\eta_h)...A(\eta_1)$. Let $(\bar{a}_0, \bar{b}_0, \bar{c}_0, \bar{d}_0, \bar{e}_0, \bar{f}_0, \bar{g}_0, \bar{l}_0) = (0, 1, 0, 1, 0, 1, 0, 1)$ and

$$\begin{pmatrix} e^{i\beta_h}g_h(x_1)\bar{a}_k \\ e^{i\beta_h}g_h(x_1)\bar{b}_k \\ e^{i\beta_h}e_h(x_2)\bar{c}_k \\ e^{i\beta_h}e_h(x_2)\bar{d}_k \\ g_h(x_1)\bar{e}_k \\ g_h(x_1)\bar{f}_k \\ f_h(x_2)\bar{g}_k \\ f_h(x_2)\bar{l}_k \end{pmatrix} = A(\zeta_k)...A(\zeta_1)\begin{pmatrix} 0 \\ e^{i\beta_h}g_h(x_1) \\ 0 \\ e^{i\beta_h}e_h(x_2) \\ 0 \\ g_h(x_1) \\ 0 \\ f_h(x_2) \end{pmatrix}$$

for $k = 1, \dots, h$. The recurrence formula of $\bar{d}_k(x_1)$ is defined by $\bar{d}_0(x_1) = 1$, $\bar{d}_1(x_1) = x_1$, and for $k = 2, \dots, h$,

$$\bar{d}_k(x_1) = x(1 + e^{-i(\eta_k-\eta_{k-1})})\bar{d}_{k-1}(x_1) - e^{-i(\eta_k-\eta_{k-1})}\bar{d}_{k-2}(x_1),$$

with $x_1 = \cos(\frac{\omega_1}{2})$, and the recurrence formula of $\bar{l}_k(x_1)$ is defined by $\bar{l}_0(x_1) = 1$, $\bar{l}_1(x_1) = x_1$ and for $k = 2, \dots, h$:

$$\bar{l}_k(x_1) = x_1(1 + e^{-i(\eta_k-\eta_{k-1})})\bar{l}_{k-1}(x_1) - e^{-i(\eta_k-\eta_{k-1})}\bar{l}_{k-2}(x_1).$$

The recurrence formula of $\bar{b}_k(x_2)$ is defined by $\bar{b}_0(x_2) = 1$, $\bar{b}_1(x_2) = x_2$, and for $k = 2, \dots, h$,

$$\bar{b}_k(x_2) = x_2(1 + e^{-i(\eta_k-\eta_{k-1})})\bar{b}_{k-1}(x_2) - e^{-i(\eta_k-\eta_{k-1})}\bar{b}_{k-2}(x_2),$$

with $x_2 = \cos(\frac{\omega_2}{2})$, and the recurrence formula of $\bar{f}_k(x_2)$ is defined by $\bar{f}_0(x_2) = 1$, $\bar{f}_1(x_2) = x_2$ and for $k = 2, \dots, h$:

$$\bar{f}_k(x_2) = x_2(1 + e^{-i(\eta_k-\eta_{k-1})})\bar{f}_{k-1}(x_2) - e^{-i(\eta_k-\eta_{k-1})}\bar{f}_{k-2}(x_2).$$

By Lemma 1, when

$$\eta_{k+1} - \eta_k = (-1)^k\pi - 2\text{arccot}\left(\tan\left(\frac{k\pi}{h}\right)\sqrt{1-\gamma^2}\right), \tag{B12}$$

with $\gamma^{-1} = \cos[\frac{1}{h}\arccos(\frac{1}{\sqrt{\epsilon}})]$ for $k = 1, 2, \dots, h-1$, we have

$$\bar{d}_h(x_1) = \bar{l}_h(x_1) = \frac{T_h\left(\frac{x_1}{\gamma}\right)}{T_h\left(\frac{1}{\gamma}\right)}, \quad \bar{b}_h(x_2) = \bar{f}_h(x_2) = \frac{T_h\left(\frac{x_2}{\gamma}\right)}{T_h\left(\frac{1}{\gamma}\right)},$$

with $T_h(\frac{1}{\gamma}) = \frac{1}{\sqrt{\epsilon}}$. Moreover, $\bar{a}_h(x_2)$, $\bar{c}_h(x_1)$, $\bar{e}_h(x_2)$, and $\bar{g}_h(x_1)$ are determined by $|\bar{a}_h(x_2)|^2 + |\bar{b}_h(x_2)|^2 = 1$, $|\bar{c}_h(x_1)|^2 + |\bar{c}_h(x_1)|^2 = 1$, $|\bar{e}_h(x_2)|^2 + |\bar{e}_h(x_2)|^2 = 1$, and $|\bar{g}_h(x_1)|^2 + |\bar{l}_h(x_1)|^2 = 1$, respectively. Hence, the result state is

$$\frac{1}{\sqrt{2}}\begin{pmatrix} e^{i\beta_h}g_h(x_1)\bar{a}_h(x_2)\\ e^{i\beta_h}g_h(x_1)\bar{b}_h(x_2)\\ e^{i\beta_h}e_h(x_2)\bar{c}_h(x_1)\\ e^{i\beta_h}e_h(x_2)\bar{d}_h(x_1)\\ g_h(x_1)\bar{e}_h(x_2)\\ g_h(x_1)\bar{f}_h(x_2)\\ f_h(x_2)\bar{g}_h(x_1)\\ f_h(x_2)\bar{l}_h(x_1)\end{pmatrix}.$$

Stage ④: Perform the final operation S. The final state is

$$\frac{1}{\sqrt{2}}\begin{pmatrix} e^{i\beta_h}e_h(x_2)\bar{c}_h(x_1)\\ f_h(x_2)\bar{g}_h(x_1)\\ e^{i\beta_h}g_h(x_1)\bar{a}_h(x_2)\\ g_h(x_1)\bar{e}_h(x_2)\\ e^{i\beta_h}e_h(x_2)\bar{d}_h(x_1)\\ f_h(x_2)\bar{l}_h(x_1)\\ e^{i\beta_h}g_h(x_1)\bar{b}_h(x_2)\\ g_h(x_1)\bar{f}_h(x_2)\end{pmatrix}.$$

Hence, the success probability P_h is

$$\begin{aligned} P_h &= 1 - \frac{1}{2}|f_h(x_2)\bar{l}_h(x_1)|^2 - \frac{1}{2}|g_h(x_1)\bar{f}_h(x_2)|^2 = 1 - \epsilon^2T_h^2\left(\frac{x_1}{\gamma}\right)T_h^2\left(\frac{x_2}{\gamma}\right)\\ &= 1 - \epsilon^2T_h^2\left(\cos\left(\frac{1}{h}\arccos\left(\frac{1}{\sqrt{\epsilon}}\right)\right)\sqrt{1-\frac{n_l}{N_l}}\right)T_h^2\left(\cos\left(\frac{1}{h}\arccos\left(\frac{1}{\sqrt{\epsilon}}\right)\right)\sqrt{1-\frac{n_r}{N_r}}\right).\end{aligned}$$

By Eqs. (B7) and (B9)–(B12), α_k, β_k can be chosen such that

$$\alpha_k = -\beta_{h+2-k} = \pi + (\eta_{k+1} - \eta_k) = 2\text{arccot}\left(\tan\left(\frac{k\pi}{h}\right)\sqrt{1-\gamma^2}\right)$$

for $k = 2, 4, \dots, h-1$, and

$$\alpha_k = -\beta_{h-k} = \pi - (\zeta_{k+1} - \zeta_k) = 2\text{arccot}\left(\tan\left(\frac{(k-1)\pi}{h}\right)\sqrt{1-\gamma^2}\right)$$

for $k = 3, 5, \dots, h$. In addition, α_1 and β_h can be any value.

2. Case 2: *h* is an even integer

First, we set

$$\beta_k = -\alpha_{h+1-k} \qquad k = 1, 2, \dots, h-1. \tag{B13}$$

Then $|\Psi_h\rangle$ reduces to

$$|\Psi_h\rangle \sim R(\beta_h)[A(\phi_{h-1})...A(\phi_1)]R(\alpha_1)S[A(\psi_{h+1})...A(\psi_1)]\,|\bar{0}\rangle\,, \tag{B14}$$

which will be proven in Appendix D by using Eqs. (B1)–(B6). Here $\phi_k = \phi_{h-k}$ for $k = 1, 2, \dots, h-1$, $\psi_k = \psi_{h+2-k}$ for $k = 1, 2, \dots, h+1$, and

$$\phi_{k+1} - \phi_k = \begin{cases} \pi - \alpha_{k+1} & k = 2, 4, \dots, h-2 \\ -\pi + \alpha_{h-k} & k = 1, 3, \dots, h-3, \end{cases} \tag{B15}$$

$$\psi_{k+1} - \psi_k = \begin{cases} \pi - \alpha_k & k = 2, 4, \dots, h-2 \\ -\pi + \alpha_{h-k+1} & k = 1, 3, \dots, h. \end{cases} \tag{B16}$$

The final state of Eq. (B14) is given by the four stages as follows:

$$\frac{1}{\sqrt{2}}\begin{pmatrix}0\\0\\0\\0\\0\\1\\0\\1\end{pmatrix} \xrightarrow[①]{A(\psi_{h+1})...A(\psi_1)} \frac{1}{\sqrt{2}}\begin{pmatrix}0\\0\\0\\0\\e_{h+1}(x_2)\\f_{h+1}(x_2)\\g_{h+1}(x_1)\\l_{h+1}(x_1)\end{pmatrix} \xrightarrow[②]{R(\alpha_1)S} \frac{1}{\sqrt{2}}\begin{pmatrix}0\\g_{h+1}(x_1)\\0\\e_{h+1}(x_2)\\0\\l_{h+1}(x_1)\\0\\f_{h+1}(x_2)\end{pmatrix}$$

$$\xrightarrow[③]{A(\phi_{h-1})...A(\phi_1)} \frac{1}{\sqrt{2}}\begin{pmatrix}g_{h+1}(x_1)\bar{a}_{h-1}(x_2)\\g_{h+1}(x_1)\bar{b}_{h-1}(x_2)\\e_{h+1}(x_2)\bar{c}_{h-1}(x_1)\\e_{h+1}(x_2)\bar{d}_{h-1}(x_1)\\l_{h+1}(x_1)\bar{e}_{h-1}(x_2)\\l_{h+1}(x_1)\bar{f}_{h-1}(x_2)\\f_{h+1}(x_2)\bar{g}_{h-1}(x_1)\\f_{h+1}(x_2)\bar{l}_{h-1}(x_1)\end{pmatrix}$$

$$\xrightarrow[④]{R(\beta_h)} \frac{1}{\sqrt{2}}\begin{pmatrix}e^{i\beta_h}g_{h+1}(x_1)\bar{a}_{h-1}(x_2)\\g_{h+1}(x_1)\bar{b}_{h-1}(x_2)\\e^{i\beta_h}e_{h+1}(x_2)\bar{c}_{h-1}(x_1)\\e_{h+1}(x_2)\bar{d}_{h-1}(x_1)\\e^{i\beta_h}l_{h+1}(x_1)\bar{e}_{h-1}(x_2)\\l_{h+1}(x_1)\bar{f}_{h-1}(x_2)\\e^{i\beta_h}f_{h+1}(x_2)\bar{g}_{h-1}(x_1)\\f_{h+1}(x_2)\bar{l}_{h-1}(x_1)\end{pmatrix}.$$

Stage ①: Apply $A(\psi_{h+1})...A(\psi_1)$ to the initial state. Let

$$(a_0, b_0, c_0, d_0, e_0, f_0, g_0, l_0) = (0, 0, 0, 0, 0, 1, 0, 1)$$

and

$$\begin{pmatrix}a_k\\b_k\\c_k\\d_k\\e_k\\f_k\\g_k\\l_k\end{pmatrix} = A(\psi_k)...A(\psi_1)\begin{pmatrix}0\\0\\0\\0\\0\\1\\0\\1\end{pmatrix}$$

for $k = 1, 2, \dots, h$. By the property of the matrix $A(\zeta_i)$, we have $a_k = b_k = c_k = d_k = 0$ for all k, and e_k, f_k, g_k, l_k can be gotten in the following. The recurrence formula of $l_k(x_1)$ is defined by $l_0(x_1) = 1$, $l_1(x_1) = x_1$ and for $k = 2, \dots, h+1$,

$$l_k(x_1) = x_1(1 + e^{-i(\psi_k - \psi_{k-1})})l_{k-1}(x_1) - e^{-i(\psi_k - \psi_{k-1})}l_{k-2}(x_1),$$

with $x_1 = \cos(\frac{\omega_1}{2})$, and the recurrence formula of $f_k(x_2)$ is defined by $f_0(x_2) = 1$, $f_1(x_2) = x_2$ and for $k = 2, \ldots, h+1$,

$$f_k(x_2) = x_2(1 + e^{-i(\psi_k - \psi_{k-1})})f_{k-1}(x_2) - e^{-i(\psi_k - \psi_{k-1})}f_{k-2}(x_2),$$

with $x_2 = \cos(\frac{\omega_2}{2})$. By Lemma 1, when

$$\psi_{k+1} - \psi_k = (-1)^k\pi - 2\mathrm{arccot}\left(\tan\left(\frac{k\pi}{h+1}\right)\sqrt{1-\gamma_1^2}\right), \tag{B17}$$

with $\gamma_1^{-1} = \cos(\frac{1}{h+1}\arccos(\frac{1}{\sqrt{\epsilon}}))$ for $k = 1, 2, \ldots, h$, we have

$$l_{h+1}(x_1) = \frac{T_{h+1}\left(\frac{x_1}{\gamma_1}\right)}{T_{h+1}\left(\frac{1}{\gamma_1}\right)}, \quad f_{h+1}(x_2) = \frac{T_{h+1}\left(\frac{x_2}{\gamma_1}\right)}{T_{h+1}\left(\frac{1}{\gamma_1}\right)},$$

with $T_{h+1}(\frac{1}{\gamma_1}) = \frac{1}{\sqrt{\epsilon}}$. Moreover, $e_{h+1}(x_2)$ and $g_{h+1}(x_1)$ are determined by $|e_{h+1}(x_2)|^2 + |f_{h+1}(x_2)|^2 = 1$ and $|g_{h+1}(x_1)|^2 + |l_{h+1}(x_1)|^2 = 1$, respectively. Therefore, the state after $A(\psi_h)\ldots A(\psi_1)$ applied to the initial state is

$$\frac{1}{\sqrt{2}}\begin{pmatrix} 0 \\ 0 \\ 0 \\ 0 \\ e_{h+1}(x_2) \\ f_{h+1}(x_2) \\ g_{h+1}(x_1) \\ l_{h+1}(x_1) \end{pmatrix}.$$

Stage ②: Apply $R(\alpha_1)S$ to the above state. After that, the state is

$$\frac{1}{\sqrt{2}}\begin{pmatrix} 0 \\ g_{h+1}(x_1) \\ 0 \\ e_{h+1}(x_2) \\ 0 \\ l_{h+1}(x_1) \\ 0 \\ f_{h+1}(x_2) \end{pmatrix}.$$

Stage ③: Perform $A(\phi_{h-1})\ldots A(\phi_1)$. Let $(\bar{a}_0, \bar{b}_0, \bar{c}_0, \bar{d}_0, \bar{e}_0, \bar{f}_0, \bar{g}_0, \bar{l}_0) = (0, 1, 0, 1, 0, 1, 0, 1)$ and

$$\frac{1}{\sqrt{2}}\begin{pmatrix} g_{h+1}(x_1)\bar{a}_k \\ g_{h+1}(x_1)\bar{b}_k \\ e_{h+1}(x_2)\bar{c}_k \\ e_{h+1}(x_2)\bar{d}_k \\ l_{h+1}(x_1)\bar{e}_k \\ l_{h+1}(x_1)\bar{f}_k \\ f_{h+1}(x_2)\bar{g}_k \\ f_{h+1}(x_2)\bar{l}_k \end{pmatrix} = A(\phi_k)\ldots A(\phi_1)\frac{1}{\sqrt{2}}\begin{pmatrix} 0 \\ g_{h+1}(x_1) \\ 0 \\ e_{h+1}(x_2) \\ 0 \\ l_{h+1}(x_1) \\ 0 \\ f_{h+1}(x_2) \end{pmatrix}$$

for $k = 1, \ldots, h-1$. The recurrence formula of $\bar{d}_k(x_1)$ is defined by $\bar{d}_0(x_1) = 1$, $\bar{d}_1(x_1) = x_1$ and for $k = 2, \ldots, h-1$,

$$\bar{d}_k(x_1) = x(1 + e^{-i(\phi_k - \phi_{k-1})})\bar{d}_{k-1}(x_1) - e^{-i(\phi_k - \phi_{k-1})}\bar{d}_{k-2}(x_1),$$

with $x_1 = \cos(\frac{\omega_1}{2})$, and the recurrence formula of $\bar{l}_k(x_1)$ is defined by $\bar{l}_0(x_1) = 1$, $\bar{l}_1(x_1) = x_1$ and for $k = 2, \ldots, h-1$:

$$\bar{l}_k(x_1) = x_1(1 + e^{-i(\phi_k - \phi_{k-1})})\bar{l}_{k-1}(x_1) - e^{-i(\phi_k - \phi_{k-1})}\bar{l}_{k-2}(x_1).$$

The recurrence formula of $\bar{b}_k(x_2)$ is defined by $\bar{b}_0(x_2) = 1$, $\bar{b}_1(x_2) = x_2$ and for $k = 2, \ldots, h-1$,

$$\bar{b}_k(x_2) = x_2(1 + e^{-i(\phi_k - \phi_{k-1})})\bar{b}_{k-1}(x_2) - e^{-i(\phi_k - \phi_{k-1})}\bar{b}_{k-2}(x_2),$$

with $x_2 = \cos(\frac{\omega_2}{2})$, and the recurrence formula of $\bar{f}_k(x_2)$ is defined by $\bar{f}_0(x_2) = 1$, $\bar{f}_1(x_2) = x_2$ and for $k = 2, \ldots, h-1$:

$$\bar{f}_k(x_2) = x_2(1 + e^{-i(\phi_k - \phi_{k-1})})\bar{f}_{k-1}(x_2) - e^{-i(\phi_k - \phi_{k-1})}\bar{f}_{k-2}(x_2).$$

By Lemma 1, when

$$\phi_{k+1} - \phi_k = (-1)^k\pi - 2\mathrm{arccot}\left[\tan\left(\frac{k\pi}{h-1}\right)\sqrt{1-\gamma_2^2}\right], \tag{B18}$$

with $\gamma_2^{-1} = \cos[\frac{1}{h-1}\arccos(\frac{1}{\sqrt{\epsilon}})]$ for $k = 1, 2, \dots, h-2$, we have

$$\bar{d}_{h-1}(x_1) = \bar{l}_{h-1}(x_1) = \frac{T_{h-1}\left(\frac{x_1}{\gamma_2}\right)}{T_{h-1}\left(\frac{1}{\gamma_2}\right)}, \quad \bar{b}_{h-1}(x_2) = \bar{f}_{h-1}(x_2) = \frac{T_{h-1}\left(\frac{x_2}{\gamma_2}\right)}{T_{h-1}\left(\frac{1}{\gamma_2}\right)},$$

with $T_{h-1}(\frac{1}{\gamma_2}) = \frac{1}{\sqrt{\epsilon}}$. Moreover, $\bar{a}_h(x_2)$, $\bar{c}_h(x_1)$, $\bar{e}_h(x_2)$, and $\bar{g}_h(x_1)$ are determined by $|\bar{a}_h(x_2)|^2 + |\bar{b}_h(x_2)|^2 = 1$, $|\bar{c}_h(x_1)|^2 + |\bar{d}_h(x_1)|^2 = 1$, $|\bar{e}_h(x_2)|^2 + |\bar{f}_h(x_2)|^2 = 1$, and $|\bar{g}_h(x_1)|^2 + |\bar{l}_h(x_1)|^2 = 1$, respectively. Hence, the result state is

$$\frac{1}{\sqrt{2}}\begin{pmatrix} g_{h+1}(x_1)\bar{a}_{h-1}(x_2) \\ g_{h+1}(x_1)\bar{b}_{h-1}(x_2) \\ e_{h+1}(x_2)\bar{c}_{h-1}(x_1) \\ e_{h+1}(x_2)\bar{d}_{h-1}(x_1) \\ l_{h+1}(x_1)\bar{e}_{h-1}(x_2) \\ l_{h+1}(x_1)\bar{f}_{h-1}(x_2) \\ f_{h+1}(x_2)\bar{g}_{h-1}(x_1) \\ f_{h+1}(x_2)\bar{l}_{h-1}(x_1) \end{pmatrix}.$$

Stage ④: Perform the final operation $R(\beta_h)$. The final state is

$$\frac{1}{\sqrt{2}}\begin{pmatrix} e^{i\beta_h} g_{h+1}(x_1)\bar{a}_{h-1}(x_2) \\ g_{h+1}(x_1)\bar{b}_{h-1}(x_2) \\ e^{i\beta_h} e_{h+1}(x_2)\bar{c}_{h-1}(x_1) \\ e_{h+1}(x_2)\bar{d}_{h-1}(x_1) \\ e^{i\beta_h} l_{h+1}(x_1)\bar{e}_{h-1}(x_2) \\ l_{h+1}(x_1)\bar{f}_{h-1}(x_2) \\ e^{i\beta_h} f_{h+1}(x_2)\bar{g}_{h-1}(x_1) \\ f_{h+1}(x_2)\bar{l}_{h-1}(x_1) \end{pmatrix}.$$

Therefore, the success probability P_h is

$$\begin{aligned} P_h &= 1 - \frac{1}{2}|c_{h+1}(x_1)d_{h-1}(x_2)|^2 - \frac{1}{2}|c_{h+1}(x_2)d_{h-1}(x_1)|^2 \\ &= 1 - \frac{\epsilon^2}{2}\left(T_{h+1}^2\left(\frac{x_1}{\gamma_1}\right)T_{h-1}^2\left(\frac{x_2}{\gamma_2}\right) + T_{h+1}^2\left(\frac{x_2}{\gamma_1}\right)T_{h-1}^2\left(\frac{x_1}{\gamma_2}\right)\right) \\ &= 1 - \frac{\epsilon^2}{2}\left[T_{h+1}^2\left(\cos\left(\frac{1}{h+1}\arccos\left(\frac{1}{\sqrt{\epsilon}}\right)\right)\sqrt{1-\frac{n_l}{N_l}}\right)\right. \\ &\quad \times T_{h-1}^2\left(\cos\left(\frac{1}{h-1}\arccos\left(\frac{1}{\sqrt{\epsilon}}\right)\right)\sqrt{1-\frac{n_r}{N_r}}\right) \\ &\quad + T_{h+1}^2\left(\cos\left(\frac{1}{h+1}\arccos\left(\frac{1}{\sqrt{\epsilon}}\right)\right)\sqrt{1-\frac{n_r}{N_r}}\right) \\ &\quad \left.\times T_{h-1}^2\left(\cos\left(\frac{1}{h-1}\arccos\left(\frac{1}{\sqrt{\epsilon}}\right)\right)\sqrt{1-\frac{n_l}{N_l}}\right)\right]. \end{aligned}$$

By Eqs. (B13) and (B15)–(B18), α_k, β_k can be chosen such that

$$\alpha_k = -\beta_{h+1-k} = \pi - (\phi_k - \phi_{k-1}) = 2\text{arccot}\left(\tan\left(\frac{k\pi}{h+1}\right)\sqrt{1-\gamma_2^2}\right)$$

for $k = 2, 4, \dots, h$, and

$$\alpha_k = -\beta_{h+1-k} = \pi - (\psi_{k+1} - \psi_k) = 2\text{arccot}\left(\tan\left(\frac{(k-1)\pi}{h-1}\right)\sqrt{1-\gamma_1^2}\right)$$

for $k = 3, 5, \dots, h-1$. In addition, α_1 and β_h can be any value.

APPENDIX C: PROOF OF EQUATIONS (13) AND (A2)

In this Appendix, we give the detailed proof of Eqs. (13) and (A2).
Recall that

$$|\Psi_h\rangle = U(\alpha_h, \beta_h)\dots U(\alpha_1, \beta_1)|\Psi_0\rangle = SC(\alpha_h)Q(\beta_h)\dots SC(\alpha_1)Q(\beta_1)|\Psi_0\rangle.$$

Using $SS = I$, we have

$$|\Psi_h\rangle = SC(\alpha_h)Q(\beta_h)\ldots SC(\alpha_1)Q(\beta_1)SS\,|\Psi_0\rangle\,.$$

Using Eqs. (6) and (7), we have

$$|\Psi_h\rangle \sim SA\left(\frac{\pi}{2}\right)R(\alpha_h)A\left(-\frac{\pi}{2}\right)SR(\beta_h)A\left(\frac{\pi}{2}\right)R(\alpha_{h-1})A\left(-\frac{\pi}{2}\right)SR(\beta_{h-1})\ldots$$
$$A\left(\frac{\pi}{2}\right)R(\alpha_2)A\left(-\frac{\pi}{2}\right)SR(\beta_2)A\left(\frac{\pi}{2}\right)R(\alpha_1)A\left(-\frac{\pi}{2}\right)SR(\beta_1)S\,|\Psi_0\rangle\,.$$

The number of S is $h+2$. Two cases need to be considered.

Case 1: h is odd. By Eq. (11), we have

$$\begin{aligned}
|\Psi_h\rangle &\sim SA\left(\frac{\pi}{2}\right)R(\alpha_h)A\left(-\frac{\pi}{2}\right)\ldots SR(\beta_{\frac{h+5}{2}})A\left(\frac{\pi}{2}\right)R(\alpha_{\frac{h+3}{2}})A\left(-\frac{\pi}{2}\right)\\
&\quad\times\left\{SR(\beta_{\frac{h+3}{2}})A\left(\frac{\pi}{2}\right)R(\alpha_{\frac{h+1}{2}})A\left(-\frac{\pi}{2}\right)SR(\beta_{\frac{h+1}{2}})A\left(\frac{\pi}{2}\right)R(\alpha_{\frac{h-1}{2}})A\left(-\frac{\pi}{2}\right)S\right\}\\
&\quad\times R(\beta_{\frac{h-1}{2}})A\left(\frac{\pi}{2}\right)R(\alpha_{\frac{h-3}{2}})A\left(-\frac{\pi}{2}\right)\ldots SR(\beta_2)A\left(\frac{\pi}{2}\right)R(\alpha_1)A\left(-\frac{\pi}{2}\right)SR(\beta_1)S\,|\Psi_0\rangle\\
&= SA\left(\frac{\pi}{2}\right)R(\alpha_h)A\left(-\frac{\pi}{2}\right)\ldots SR(\beta_{\frac{h+5}{2}})A\left(\frac{\pi}{2}\right)R(\alpha_{\frac{h+3}{2}})A\left(-\frac{\pi}{2}\right)\\
&\quad\times\left\{R(\beta_{\frac{h+1}{2}})A\left(\frac{\pi}{2}\right)R(\alpha_{\frac{h-1}{2}})A\left(-\frac{\pi}{2}\right)SR(\beta_{\frac{h+3}{2}})A\left(\frac{\pi}{2}\right)R(\alpha_{\frac{h+1}{2}})A\left(-\frac{\pi}{2}\right)\right\}\\
&\quad\times R(\beta_{\frac{h-1}{2}})A\left(\frac{\pi}{2}\right)R(\alpha_{\frac{h-3}{2}})A\left(-\frac{\pi}{2}\right)\ldots SR(\beta_2)A\left(\frac{\pi}{2}\right)R(\alpha_1)A\left(-\frac{\pi}{2}\right)SR(\beta_1)S\,|\Psi_0\rangle\\
&= SA\left(\frac{\pi}{2}\right)R(\alpha_h)A\left(-\frac{\pi}{2}\right)R(\beta_{h-1})A\left(\frac{\pi}{2}\right)\ldots A\left(\frac{\pi}{2}\right)R(\alpha_1)A\left(-\frac{\pi}{2}\right)\\
&\quad\times SR(\beta_h)A\left(\frac{\pi}{2}\right)R(\alpha_{h-1})A\left(-\frac{\pi}{2}\right)\ldots R(\alpha_2)A\left(-\frac{\pi}{2}\right)R(\beta_1)S\,|\Psi_0\rangle\,.
\end{aligned}$$

The process is as follows. We first select the formula

$$\left\{SR(\beta_{\frac{h+3}{2}})A\left(\frac{\pi}{2}\right)R(\alpha_{\frac{h+1}{2}})A\left(-\frac{\pi}{2}\right)SR(\beta_{\frac{h+1}{2}})A\left(\frac{\pi}{2}\right)R(\alpha_{\frac{h-1}{2}})A\left(-\frac{\pi}{2}\right)S\right\},$$

containing the middle S, and then this formula reduces to

$$\left\{R(\beta_{\frac{h+1}{2}})A\left(\frac{\pi}{2}\right)R(\alpha_{\frac{h-1}{2}})A\left(-\frac{\pi}{2}\right)SR(\beta_{\frac{h+3}{2}})A\left(\frac{\pi}{2}\right)R(\alpha_{\frac{h+1}{2}})A\left(-\frac{\pi}{2}\right)\right\},$$

according to Eq. (11). The final result can be obtained after repeating the above steps. Using Eq. (10) and $A(-\frac{\pi}{2})A(\frac{\pi}{2}) = I$, we have

$$\begin{aligned}
|\Psi_h\rangle &\sim SA\left(\frac{\pi}{2}\right)R(\alpha_h)A\left(-\frac{\pi}{2}\right)R(\beta_{h-1})A\left(\frac{\pi}{2}\right)\ldots A\left(\frac{\pi}{2}\right)R(\alpha_1)A\left(-\frac{\pi}{2}\right)\\
&\quad\times SR(\beta_h)A\left(\frac{\pi}{2}\right)R(\alpha_{h-1})A\left(-\frac{\pi}{2}\right)\ldots R(\alpha_2)A\left(-\frac{\pi}{2}\right)R(\beta_1)SA\left(\frac{\pi}{2}\right)SA\left(\frac{\pi}{2}\right)|\bar{0}\rangle\\
&\sim SA\left(\frac{\pi}{2}\right)R(\alpha_h)A\left(-\frac{\pi}{2}\right)R(\beta_{h-1})A\left(\frac{\pi}{2}\right)\ldots R(\beta_2)A\left(\frac{\pi}{2}\right)R(\alpha_1)\\
&\quad\times SR(\beta_h)A\left(\frac{\pi}{2}\right)R(\alpha_{h-1})A\left(-\frac{\pi}{2}\right)\ldots R(\alpha_2)A\left(-\frac{\pi}{2}\right)R(\beta_1)A\left(\frac{\pi}{2}\right)|\bar{0}\rangle\,.
\end{aligned}$$

Here, two cases need to be discussed.

Case 1.1: When $h \bmod 4 = 1$, $\beta_i = \alpha_{h+2-i}$ for $i = 2, 4, \ldots, h-1$, and $\beta_i = \alpha_{h-i}$ for $i = 1, 3, \ldots, h-2$, using Eqs. (8) and (9), we have

$$|\Psi_h\rangle \sim SA\left(\frac{\pi}{2}\right)A\left(-\frac{\pi}{2}+\alpha_h\right)A\left(\frac{\pi}{2}-\alpha_3+\alpha_h\right)A\left(-\frac{\pi}{2}-\alpha_3+\alpha_h+\alpha_{h-2}\right)$$

$$\begin{aligned}&\ldots A\left(\frac{\pi}{2}-\alpha_3-\alpha_5\cdots-\alpha_{k_1}+\alpha_{k_1+2}\cdots+\alpha_h\right)\\&\ldots A\left(-\frac{\pi}{2}-\alpha_3+\alpha_h+\alpha_{h-2}\right)A\left(\frac{\pi}{2}-\alpha_3+\alpha_h\right)A\left(-\frac{\pi}{2}+\alpha_h\right)A\left(\frac{\pi}{2}\right)R(\alpha_1)\\&SR(\beta_h)A\left(\frac{\pi}{2}\right)A\left(-\frac{\pi}{2}+\alpha_{h-1}\right)A\left(\frac{\pi}{2}-\alpha_2+\alpha_{h-1}\right)A\left(-\frac{\pi}{2}-\alpha_2+\alpha_{h-1}+\alpha_{h-3}\right)\\&\ldots A\left(\frac{\pi}{2}-\alpha_2-\alpha_4\cdots-\alpha_{k_2}+\alpha_{k_2+2}\cdots+\alpha_{h-1}\right)\\&\ldots A\left(-\frac{\pi}{2}-\alpha_2+\alpha_{h-1}+\alpha_{h-3}\right)A\left(\frac{\pi}{2}-\alpha_2+\alpha_{h-1}\right)A\left(-\frac{\pi}{2}+\alpha_{h-1}\right)A\left(\frac{\pi}{2}\right)|\bar{0}\rangle,\end{aligned} \tag{C1}$$

where $k_1=(h+1)/2$, $k_2=(h-1)/2$.

Case 1.2: When $h \bmod 4=3$, $\beta_i=\alpha_{h+2-i}$ for $i=2,4,\ldots,h-1$, and $\beta_i=\alpha_{h-i}$ for $i=1,3,\ldots,h-2$, using Eqs. (8) and (9), we have

$$\begin{aligned}|\Psi_h\rangle\sim\, &SA\left(\frac{\pi}{2}\right)A\left(-\frac{\pi}{2}+\alpha_h\right)A\left(\frac{\pi}{2}-\alpha_3+\alpha_h\right)A\left(-\frac{\pi}{2}-\alpha_3+\alpha_h+\alpha_{h-2}\right)\\&\ldots A\left(-\frac{\pi}{2}-\alpha_3-\alpha_5\cdots-\alpha_{k_1}+\alpha_{k_1+2}\cdots+\alpha_h\right)\\&\ldots A\left(-\frac{\pi}{2}-\alpha_3+\alpha_h+\alpha_{h-2}\right)A\left(\frac{\pi}{2}-\alpha_3+\alpha_h\right)A\left(-\frac{\pi}{2}+\alpha_h\right)A\left(\frac{\pi}{2}\right)R(\alpha_1)\\&SR(\beta_h)A\left(\frac{\pi}{2}\right)A\left(-\frac{\pi}{2}+\alpha_{h-1}\right)A\left(\frac{\pi}{2}-\alpha_2+\alpha_{h-1}\right)A\left(-\frac{\pi}{2}-\alpha_2+\alpha_{h-1}+\alpha_{h-3}\right)\\&\ldots A\left(-\frac{\pi}{2}-\alpha_2-\alpha_4\cdots-\alpha_{k_2}+\alpha_{k_2+2}\cdots+\alpha_{h-1}\right)\\&\ldots A\left(-\frac{\pi}{2}-\alpha_2+\alpha_{h-1}+\alpha_{h-3}\right)A\left(\frac{\pi}{2}-\alpha_2+\alpha_{h-1}\right)A\left(-\frac{\pi}{2}+\alpha_{h-1}\right)A\left(\frac{\pi}{2}\right)|\bar{0}\rangle,\end{aligned} \tag{C2}$$

where $k_1=(h-1)/2$, $k_2=(h-3)/2$.

Thus, we can get Eq. (13) by rewriting Eqs. (C1) and (C2) as follows:

$$|\Psi_h\rangle\sim S[A(\eta_h)...A(\eta_1)]R(\alpha_1)SR(\beta_h)[A(\zeta_h)...A(\zeta_1)]\,|\bar{0}\rangle, \tag{13}$$

where $\eta_k=\eta_{h+1-k}$ and $\zeta_k=\zeta_{h+1-k}$ for $k=1,2,\ldots,h$, and

$$\eta_{k+1}-\eta_k=\begin{cases}\pi-\alpha_{k+1} & k=2,4,\ldots,h-1\\ -\pi+\alpha_{h-k+1} & k=3,5,\ldots,h,\end{cases}$$

$$\zeta_{k+1}-\zeta_k=\begin{cases}\pi-\alpha_{k} & k=2,4,\ldots,h-1\\ -\pi+\alpha_{h-k} & k=3,5,\ldots,h.\end{cases}$$

Here, when $h \bmod 4=1$,

$$\eta_{(h+1)/2}=\frac{\pi}{2}+(\alpha_{(h+5)/2}+\alpha_{(h+9)/2}+\cdots+\alpha_{h-2}+\alpha_h)-(\alpha_3+\alpha_5+\cdots+\alpha_{(h-3)/2}+\alpha_{(h+1)/2}),$$

$$\zeta_{(h+1)/2}=\frac{\pi}{2}+(\alpha_{(h+3)/2}+\alpha_{(h+7)/2}+\cdots+\alpha_{h-3}+\alpha_{h-1})-(\alpha_2+\alpha_4+\cdots+\alpha_{(h-5)/2}+\alpha_{(h-1)/2}),$$

and when $h \bmod 4=3$,

$$\begin{aligned}\eta_{(h+1)/2}&=-\frac{\pi}{2}+(\alpha_{(h+3)/2}+\alpha_{(h+7)/2}+\cdots+\alpha_{h-2}+\alpha_h)-(\alpha_3+\alpha_5+\cdots+\alpha_{(h-5)/2}+\alpha_{(h-1)/2}),\\ \zeta_{(h+1)/2}&=-\frac{\pi}{2}+(\alpha_{(h+1)/2}+\alpha_{(h+5)/2}+\cdots+\alpha_{h-3}+\alpha_{h-1})-(\alpha_2+\alpha_4+\cdots+\alpha_{(h-7)/2}+\alpha_{(h-3)/2}).\end{aligned}$$

Case 2: h is even. Using Eq. (11), there is

$$
\begin{aligned}
|\Psi_h\rangle \sim\ & SA\left(\frac{\pi}{2}\right)R(\alpha_h)A\left(-\frac{\pi}{2}\right)...SR(\beta_{\frac{h}{2}+2})A\left(\frac{\pi}{2}\right)R(\alpha_{\frac{h}{2}+1})A\left(-\frac{\pi}{2}\right)\\
& SR(\beta_{\frac{h}{2}+1})A\left(\frac{\pi}{2}\right)R(\alpha_{\frac{h}{2}})A\left(-\frac{\pi}{2}\right)SR(\beta_{\frac{h}{2}})A\left(\frac{\pi}{2}\right)R(\alpha_{\frac{h}{2}-1})A\left(-\frac{\pi}{2}\right)\\
& SR(\beta_{\frac{h}{2}-1})A\left(\frac{\pi}{2}\right)R(\alpha_{\frac{h}{2}-2})A\left(-\frac{\pi}{2}\right)...SR(\beta_2)A\left(\frac{\pi}{2}\right)R(\alpha_1)A\left(-\frac{\pi}{2}\right)SR(\beta_1)S\,|\Psi_0\rangle\\
=\ & SA\left(\frac{\pi}{2}\right)R(\alpha_h)A\left(-\frac{\pi}{2}\right)SR(\beta_h)A\left(\frac{\pi}{2}\right)R(\alpha_{h-1})A\left(-\frac{\pi}{2}\right)...\\
& SR(\beta_{\frac{h}{2}+2})A\left(\frac{\pi}{2}\right)R(\alpha_{\frac{h}{2}+1})A\left(-\frac{\pi}{2}\right)R(\beta_{\frac{h}{2}})A\left(\frac{\pi}{2}\right)R(\alpha_{\frac{h}{2}-1})A\left(-\frac{\pi}{2}\right)\\
& SR(\beta_{\frac{h}{2}+1})A\left(\frac{\pi}{2}\right)R(\alpha_{\frac{h}{2}})A\left(-\frac{\pi}{2}\right)R(\beta_{\frac{h}{2}-1})A\left(\frac{\pi}{2}\right)R(\alpha_{\frac{h}{2}-2})A\left(-\frac{\pi}{2}\right)S...\\
& SR(\beta_2)A\left(\frac{\pi}{2}\right)R(\alpha_1)A\left(-\frac{\pi}{2}\right)SR(\beta_1)S\,|\Psi_0\rangle\\
=\ & SA\left(\frac{\pi}{2}\right)R(\alpha_h)A\left(-\frac{\pi}{2}\right)R(\beta_{h-1})A\left(\frac{\pi}{2}\right)...A\left(\frac{\pi}{2}\right)R(\alpha_2)A\left(-\frac{\pi}{2}\right)R(\beta_1)\\
& SR(\beta_h)A\left(\frac{\pi}{2}\right)R(\alpha_{h-1})A\left(-\frac{\pi}{2}\right)...R(\alpha_1)A\left(-\frac{\pi}{2}\right)|\Psi_0\rangle\,.
\end{aligned}
$$

Using Eq. (10) and $A(-\frac{\pi}{2})A(\frac{\pi}{2}) = I$, we have

$$
\begin{aligned}
|\Psi_h\rangle \sim\ & SA\left(\frac{\pi}{2}\right)R(\alpha_h)A\left(-\frac{\pi}{2}\right)R(\beta_{h-1})A\left(\frac{\pi}{2}\right)...A\left(\frac{\pi}{2}\right)R(\alpha_2)A\left(-\frac{\pi}{2}\right)R(\beta_1)\\
& \times SR(\beta_h)A\left(\frac{\pi}{2}\right)R(\alpha_{h-1})A\left(-\frac{\pi}{2}\right)...R(\alpha_1)A\left(-\frac{\pi}{2}\right)A\left(\frac{\pi}{2}\right)SA\left(\frac{\pi}{2}\right)|\bar{0}\rangle\\
\sim\ & R(\beta_h)A\left(\frac{\pi}{2}\right)R(\alpha_{h-1})A\left(-\frac{\pi}{2}\right)...A\left(-\frac{\pi}{2}\right)R(\beta_2)A\left(\frac{\pi}{2}\right)R(\alpha_1)S\\
& \times A\left(\frac{\pi}{2}\right)R(\alpha_h)A\left(-\frac{\pi}{2}\right)R(\beta_{h-1})A\left(\frac{\pi}{2}\right)...A\left(\frac{\pi}{2}\right)R(\alpha_2)A\left(-\frac{\pi}{2}\right)R(\beta_1)A\left(\frac{\pi}{2}\right)|\bar{0}\rangle\,.
\end{aligned}
$$

Here, two cases need to be discussed.

Case 2.1: When $h \bmod 4 = 0$, and $\beta_i = \alpha_{h+1-i}$ for $i = 1, 2, \ldots, h-1$, using Eqs. (8) and (9), we have

$$
\begin{aligned}
|\Psi_h\rangle \sim\ & R(\beta_h)A\left(\frac{\pi}{2}\right)A\left(-\frac{\pi}{2}+\alpha_{h-1}\right)A\left(\frac{\pi}{2}-\alpha_3+\alpha_{h-1}\right)A\left(-\frac{\pi}{2}-\alpha_3+\alpha_{h-1}+\alpha_{h-3}\right)\\
& ...A\left(-\frac{\pi}{2}-\alpha_3-\alpha_5\cdots-\alpha_{k_1}+\alpha_{k_1+2}\cdots+\alpha_{h-1}\right)...\\
& A\left(-\frac{\pi}{2}-\alpha_3+\alpha_{h-1}+\alpha_{h-3}\right)A\left(\frac{\pi}{2}-\alpha_3+\alpha_{h-1}\right)A\left(-\frac{\pi}{2}+\alpha_{h-1}\right)A\left(\frac{\pi}{2}\right)R(\alpha_1)S\\
& A\left(\frac{\pi}{2}\right)A\left(-\frac{\pi}{2}+\alpha_h\right)A\left(\frac{\pi}{2}-\alpha_2+\alpha_h\right)A\left(-\frac{\pi}{2}-\alpha_2+\alpha_h+\alpha_{h-2}\right)\\
& ...A\left(\frac{\pi}{2}-\alpha_2-\alpha_4\cdots-\alpha_{k_2}+\alpha_{k_2+2}\cdots+\alpha_h\right)...\\
& A\left(-\frac{\pi}{2}-\alpha_2+\alpha_h+\alpha_{h-2}\right)A\left(\frac{\pi}{2}-\alpha_2+\alpha_h\right)A\left(-\frac{\pi}{2}+\alpha_h\right)A\left(\frac{\pi}{2}\right)|\bar{0}\rangle\,,
\end{aligned}
\tag{C3}
$$

where $k_1 = h/2 - 1$, $k_2 = h/2$.

Case 2.2: When h mod $4 = 2$, and $\beta_i = \alpha_{h+1-i}$ for $i = 1, 2, \ldots, h-1$, using Eqs. (8) and (9), we have

$$\begin{aligned}|\Psi_h\rangle \sim & R(\beta_h)A\left(\frac{\pi}{2}\right)A\left(-\frac{\pi}{2}+\alpha_{h-1}\right)A\left(\frac{\pi}{2}-\alpha_3+\alpha_{h-1}\right)A\left(-\frac{\pi}{2}-\alpha_3+\alpha_{h-1}+\alpha_{h-3}\right)\\ & ...A\left(\frac{\pi}{2}-\alpha_3-\alpha_5\cdots-\alpha_{k_1}+\alpha_{k_1+2}\cdots+\alpha_{h-1}\right)...\\ & A\left(-\frac{\pi}{2}-\alpha_3+\alpha_{h-1}+\alpha_{h-3}\right)A\left(\frac{\pi}{2}-\alpha_3+\alpha_{h-1}\right)A\left(-\frac{\pi}{2}+\alpha_{h-1}\right)A\left(\frac{\pi}{2}\right)R(\alpha_1)S\\ & A\left(\frac{\pi}{2}\right)A\left(-\frac{\pi}{2}+\alpha_h\right)A\left(\frac{\pi}{2}-\alpha_2+\alpha_h\right)A\left(-\frac{\pi}{2}-\alpha_2+\alpha_h+\alpha_{h-2}\right)\\ & ...A\left(-\frac{\pi}{2}-\alpha_2-\alpha_4\cdots-\alpha_{k_2}+\alpha_{k_2+2}\cdots+\alpha_h\right)...\\ & A\left(-\frac{\pi}{2}-\alpha_2+\alpha_h+\alpha_{h-2}\right)A\left(\frac{\pi}{2}-\alpha_2+\alpha_h\right)A\left(-\frac{\pi}{2}+\alpha_h\right)A\left(\frac{\pi}{2}\right)|\bar{0}\rangle\,, \end{aligned} \tag{C4}$$

where $k_1 = h/2$, $k_2 = h/2 - 1$.

Using Eqs. (C3) and (C4), we can get Eq. (A2),

$$|\Psi_h\rangle \sim R(\beta_h)[A(\phi_{h-1})...A(\phi_1)]R(\alpha_1)S[A(\psi_{h+1})...A(\psi_1)]\,|\bar{0}\rangle\,, \tag{A2}$$

where $\phi_k = \phi_{h-k}$ for $k = 1, 2, \ldots, h-1$, $\psi_k = \psi_{h+2-k}$ for $k = 1, 2, \ldots, h+1$, and

$$\phi_{k+1}-\phi_k = \begin{cases}\pi-\alpha_{k+1} & \text{for } k = 2, 4, \ldots, h-2\\ -\pi+\alpha_{h-k} & \text{for } k = 1, 3, \ldots, h-3,\end{cases}$$

$$\psi_{k+1}-\psi_k = \begin{cases}\pi-\alpha_{k} & \text{for } k = 2, 4, \ldots, h-2\\ -\pi+\alpha_{h-k+1} & \text{for } k = 1, 3, \ldots, h.\end{cases}$$

Here, when h mod $4 = 0$, there are

$$\phi_{h/2} = -\frac{\pi}{2}+(\alpha_{h/2+1}+\alpha_{h/2+3}+\cdots+\alpha_{h-3}+\alpha_{h-1})-(\alpha_3+\alpha_5+\cdots+\alpha_{h/2-3}+\alpha_{h/2-1}),$$
$$\psi_{h/2+1} = \frac{\pi}{2}+(\alpha_{h/2+2}+\alpha_{h/2+4}+\cdots+\alpha_{h-2}+\alpha_h)-(\alpha_2+\alpha_4+\cdots+\alpha_{h/2-2}+\alpha_{h/2},$$

and when h mod $4 = 2$, there are

$$\phi_{h/2} = \frac{\pi}{2}+(\alpha_{h/2+2}+\alpha_{h/2+4}+\cdots+\alpha_{h-3}+\alpha_{h-1})-(\alpha_3+\alpha_5+\cdots+\alpha_{h/2-2}+\alpha_{h/2}),$$
$$\psi_{h/2+1} = -\frac{\pi}{2}+(\alpha_{h/2+1}+\alpha_{h/2+3}+\cdots+\alpha_{h-2}+\alpha_h)-(\alpha_2+\alpha_4+\cdots+\alpha_{h/2-3}+\alpha_{h/2-1}).$$

APPENDIX D: PROOF OF EQUATIONS (B8) AND (B14)

The process of proving Eq. (13) [(A2)] uses Eqs. (6)–(11) in Appendix C. There are the same mathematical equations in two cases [see Eqs. (6)–(11) and Eqs. (B1)–(B6)], although their subspace dimensions in the analysis are different. Therefore, the proof of Eq. (B8) [Eq. (B14)] is the same as Eq. (13) [(A2)].

[1] Y. Aharonov, L. Davidovich, and N. Zagury, Quantum random walks, Phys. Rev. A **48**, 1687 (1993).

[2] A. Ambainis, Quantum walk algorithm for element distinctness, SIAM J. Comput. **37**, 210 (2007).

[3] F. Magniez, M. Santha, and M. Szegedy, Quantum algorithms for the triangle problem, SIAM J. Comput. **37**, 413 (2007).

[4] A. Montanaro, Quantum-walk speedup of backtracking algorithms, Theory Comput. **14**, 1 (2018).

[5] H. Buhrman and R. Spalek, Quantum verification of matrix products, in *Proceedings of the Seventeenth ACM-SIAM Symposium on Discrete Algorithms* (Society for Industrial and Applied Mathematics, Philadelphia, 2006), pp. 880–889.

[6] F. Magniez and A. Nayak, Quantum complexity of testing group commutativity, Algorithmica **48**, 221 (2007).

[7] A. M. Childs, L. J. Schulman, and U. V. Vazirani, Quantum algorithms for hidden nonlinear structures, in *Proceedings of the 48th IEEE Symposium on Foundations of Computer Science* (IEEE Computer Society, New York, 2007), pp. 395–404.

[8] S. Jeffery, R. Kothari, and F. Magniez, Nested quantum walks with quantum data structures, in *Proceedings of the Twenty-Fourth Annual ACM-SIAM Symposium on Discrete Algorithms* (2013), pp. 1474–1485.

[9] A. Belovs, A. M. Childs, S. Jeffery, R. Kothari, and F. Magniez, Time-efficient quantum walks for 3-distinctness, in *Proceedings*

of the 40th International Colloquium on Automata, Languages, and Programming, Lecture Notes in Computer Science, Vol. 7965 (Springer, New York, 2013), pp. 105–122.

[10] A. M. Childs, Universal Computation by Quantum Walk, Phys. Rev. Lett. **102**, 180501 (2009).

[11] N. B. Lovett, S. Cooper, M. Everitt, M. Trevers, and V. Kendon, Universal quantum computation using the discrete-time quantum walk, Phys. Rev. A **81**, 042330 (2010).

[12] F. Zähringer, G. Kirchmair, R. Gerritsma, E. Solano, R. Blatt, and C. F. Roos, Realization of a Quantum Walk With One and Two Trapped Ions, Phys. Rev. Lett. **104**, 100503 (2010).

[13] A. Peruzzo, M. Lobino, J. C. F. Matthews, N. Matsuda, A. Politi, K. Poulios, X.-Q. Zhou, Y. Lahini, N. Ismail, K. Wörhoff, Y. Bromberg, Y. Silberberg, M. G. Thompson, and J. L. OBrien, Quantum walks of correlated photons, Science **329**, 1500 (2010).

[14] C. Chen, X. Ding, J. Qin, Y. He, Y.-H. Luo, M.-C. Chen, C. Liu, X.-L. Wang, W.-J. Zhang, H. Li, L.-X. You, Z. Wang, D.-W. Wang, B. C. Sanders, C.-Y. Lu, and J.-W. Pan, Observation of Topologically Protected Edge States in a Photonic Two-Dimensional Quantum Walk, Phys. Rev. Lett. **121**, 100502 (2018).

[15] M. Gong, S. Wang, C. Zha, M.-C. Chen, H.-L. Huang, Y. Wu, Q. Zhu, Y. Zhao, S. Li, S. Guo, H. Qian, Y. Ye, F. Chen, C. Ying, J. Yu, D. Fan, D. Wu, H. Su, H. Deng, H. Rong *et al.*, Quantum walks on a programmable two-dimensional 62-qubit superconducting processor, Science **372**, 948 (2021).

[16] D. A. Meyer, From quantum cellular automata to quantum lattice gases, J. Stat. Phys. **85**, 551 (1996).

[17] D. A. Meyer, On the absence of homogeneous scalar unitary cellular automata, Phys. Lett. A **223**, 337 (1996).

[18] J. Watrous, Quantum simulations of classical random walks and undirected graph connectivity, J. Comput. Syst. Sci. **62**, 376 (2001).

[19] A. Ambainis, E. Bach, A. Nayak, A. Vishwanath, and J. Watrous, One-dimensional quantum walks, in *Proceedings of the 33rd ACM Symposium on Theory of Computing* (Association for Computing Machinery, New York, 2001), pp. 37–49.

[20] D. Aharonov, A. Ambainis, J. Kempe, and U. V. Vazirani, Quantum walks on graphs, in *Proceedings of the 33rd ACM Symposium on Theory of Computing* (Association for Computing Machinery, New York, 2001), pp. 50–59.

[21] E. Farhi and S. Gutmann, Quantum computation and decision trees, Phys. Rev. A **58**, 915 (1998).

[22] A. M. Childs, E. Farhi, and S. Gutmann, An example of the difference between quantum and classical random walks, Quantum Inf. Process. **1**, 35 (2002).

[23] N. Shenvi, J. Kempe, and K. Birgitta Whaley, Quantum random-walk search algorithm, Phys. Rev. A **67**, 052307 (2003).

[24] A. Ambainis, J. Kempe, and A. Rivosh, Coins make quantum walks faster, in *Proceedings of the Sixteenth ACM-SIAM Symposium on Discrete Algorithms* (Society for Industrial and Applied Mathematics, Philadelphia, 2005), pp. 1099–1108.

[25] M. Szegedy, Quantum speed-up of markov chain based algorithms, in *Proceedings of the 45th Symposium on Foundations of Computer Science Proceedings* (IEEE Computer Society, New York, 2004), pp. 32–41.

[26] F. Magniez, A. Nayak, J. Roland, and M. Santha, Search via quantum walk, SIAM J. Comput. **40**, 142 (2011).

[27] H. Krovi, F. Magniez, M. Ozols, and J. Roland, Quantum walks can find a marked element on any graph, Algorithmica **74**, 851 (2016).

[28] A. Ambainis, A. Gilyén, S. Jeffery, and M. Kokainis, Quadratic speedup for finding marked vertices by quantum walks, in *Proceedings of the 52nd ACM Symposium on Theory of Computing* (Association for Computing Machinery, New York, 2020), pp. 412–424.

[29] S. Apers, A. Gilyén, and S. Jeffery, A unified framework of quantum walk search, in *Proceedings of the 38th International Symposium on Theoretical Aspects of Computer Science* (Schloss Dagstuhl – Leibniz Center for Informatics, Dagstuhl, Germany, 2021), pp. 6:1–6:13.

[30] G. Brassard, Searching a quantum phone book, Science **275**, 627 (1997).

[31] Grover's quantum searching technique is like cooking a soufflé. You put the state obtained by quantum parallelism in a "quantum oven" and let the desired answer rise slowly. Success is almost guaranteed if you open the oven at just the right time. But the soufflé is very likely to fall—the amplitude of the correct answer drops to zero—if you open the oven too early. Furthermore, the soufflé could burn if you overcook it: Strangely, the amplitude of the desired state starts shrinking after reaching its maximum. After twice the optimal number of shakes, you are no more likely to succeed than before the first shake.

[32] M. Boyer, G. Brassard, P. Høyer, and A. Tapp, Tight bounds on quantum searching, Fortschr. Phys. **46**, 493 (1998).

[33] G. Brassard, P. Høyer, M. Mosca, and A. Tapp, Quantum amplitude amplification and estimation, Contemp. Math. **305**, 53 (2002).

[34] L. K. Grover, Fixed-Point Quantum Search, Phys. Rev. Lett. **95**, 150501 (2005).

[35] T. J. Yoder, G. H. Low, and I. L. Chuang, Fixed-Point Quantum Search With an Optimal Number of Queries, Phys. Rev. Lett. **113**, 210501 (2014).

[36] C. Cafaro, Geometric algebra and information geometry for quantum computational software, Physica A **470**, 154 (2017).

[37] C. Cafaro and P. M. Alsing, Continuous-time quantum search and time-dependent two-level quantum systems, Int. J. Quantum Inform. **17**, 1950025 (2019).

[38] D. Reitzner, M. Hillery, E. Feldman, and V. Bužek, Quantum searches on highly symmetric graphs, Phys. Rev. A **79**, 012323 (2009).

[39] M. L. Rhodes and T. G. Wong, Quantum walk search on the complete bipartite graph, Phys. Rev. A **99**, 032301 (2019).

[40] S. Cottrell and M. Hillery, Finding Structural Anomalies in Star Graphs Using Quantum Walks, Phys. Rev. Lett. **112**, 030501 (2014).

[41] D. Qu, S. Marsh, K. Wang, L. Xiao, J. Wang, and P. Xue, Deterministic Search on Star Graphs Via Quantum Walks, Phys. Rev. Lett. **128**, 050501 (2022).

[42] M. Abramowitz and I. A. Stegun, *Handbook of Mathematical Functions with Formulas, Graphs, and Mathematical Tables* (U.S. Government Printing Office, 1964).